AMERICAN SOCIETY FOR MICROBIOLOGY | Molecular and Cellular Biology®

RESEARCH ARTICLE

Inactivation of Cyclic AMP Response Element Transcription Caused by Constitutive p38 Activation Is Mediated by Hyperphosphorylation-Dependent CRTC2 Nucleocytoplasmic Transport

Huabin Ma,[a] Zeyuan Liu,[a] Chuan-Qi Zhong,[a] Yifei Liu,[a] Zhirong Zhang,[a] Yaoji Liang,[a] Jingxian Li,[a] Shoufa Han,[b] Jiahuai Han[a]

[a]State Key Laboratory of Cellular Stress Biology, Innovation Center for Cell Signaling Network, School of Life Sciences, Xiamen University, Xiamen, Fujian, China

[b]State Key Laboratory for Physical Chemistry of Solid Surfaces, Department of Chemical Biology, College of Chemistry and Chemical Engineering, The Key Laboratory for Chemical Biology of Fujian Province, The MOE Key Laboratory of Spectrochemical Analysis & Instrumentation, and Innovation Center for Cell Signaling Network, Xiamen University, Xiamen, China

ABSTRACT The p38 signal transduction pathway can be activated transiently or constitutively, depending on the contexts in which the activation occurs. However, the biological consequence of constitutive activation of p38 is largely unknown. After screening 300 transcriptional cofactors, we identified CRTC2 as a downstream substrate of constitutively activated p38. Constitutive, rather than transient, activation of p38 led to hyperphosphorylation of CRTC2, resulting in CRTC2 cytosolic relocation and subsequent inactivation of cyclic AMP response element (CRE)-mediated transcription. Interestingly, the cytosolic translocation of CRTC2 depended on phosphorylation accumulation at multiple sites (≥11 phosphoserine/phosphothreonine residues) but not on specific sites. The hyperphosphorylation-driven nucleocytoplasmic transport of CRTC2 may not be a rare case of nuclear export of proteins, as we also observed that constitutively activated p38 promoted FOS nuclear export in a hyperphosphorylation-dependent manner. Collectively, our study uncovered a previously unknown mechanism of inactivation of selected transcription, which results from hyperphosphorylation-driven nucleocytoplasmic transport of cofactors or transcription factors mediated by constitutively active kinase.

KEYWORDS constitutive activation, hyperphosphorylation, nucleocytoplasmic transport, p38 signaling pathway

The p38 mitogen-activated protein kinase (MAPK) subfamily, consisting of p38α, p38β, p38γ, and p38δ, plays critical roles in diverse biological processes, including cell proliferation, differentiation, senescence, inflammation, and death (1, 2). p38α is the most studied and is often referred as p38. Activation of p38 via the MAP3K-MAP2K-MAPK cascade could be triggered by a variety of extracellular stimuli ranging from inflammatory cytokines to growth factors to environmental stress (3, 4). To date, the discovery of p38 functions has been achieved mostly under transient activation signaling, whereas the regulation and biological consequences of constitutive p38 activation have been largely overlooked.

Transcription in eukaryotic cells necessitates a broad arrange of protein transcription factors (TFs), which interact with the regulatory regions of DNA (5). Many TFs encompassing a broad range of actions have been shown to be directly or indirectly phosphorylated and subsequently activated by p38; these include activating transcription factor 2 (ATF2), myocyte enhancing factor 2C (MEF2C), MEF2A, C/EBPβ, STAT1/4, p53, etc. (6, 7). Apart from TFs, transcription cofactors (TcoFs), which interact with DNA binding proteins instead of DNA, are also essential for transcription (8–10).

Citation Ma H, Liu Z, Zhong C-Q, Liu Y, Zhang Z, Liang Y, Li J, Han S, Han J. 2019. Inactivation of cyclic AMP response element transcription caused by constitutive p38 activation is mediated by hyperphosphorylation-dependent CRTC2 nucleocytoplasmic transport. Mol Cell Biol 39:e00554-18. https://doi.org/10.1128/MCB.00554-18.

Address correspondence to Jiahuai Han, jhan@xmu.edu.cn.

H.M. and Z.L. contributed equally to this article.

Received 27 November 2018
Returned for modification 14 December 2018
Accepted 1 February 2019
Accepted manuscript posted online 19 February 2019
Published 16 April 2019

The cyclic AMP (cAMP) response element (CRE)-regulated transcription coactivator (CRTC) family consists of three members (CRTC1, CRTC2, and CRTC3), which are powerful coactivators of CRE-mediated transcription, and the nuclear localization is indispensable for the coactivity (11–13). Consistent with the documented nucleocytosolic shuttle of TcoFs driven by phosphorylation, under basal conditions, CRTC2 is phosphorylated on serine 171 by the salt-inducible kinases (SIKs) and sequestered in the cytoplasm through interaction with 14-3-3 proteins. Conversely, nuclear import of CRTC2 could be triggered by dephosphorylation, a process carried out by cAMP- and calcium signal-mediated inhibition of SIKs and activation of phosphatase calcineurin (CN) (14). Dephosphorylated CRTC2 translocates to the nucleus and then binds to the bZIP domain of CREB, leading to increased CREB occupancy over cognate binding sites (13, 15). The mechanism in which the cellular localization of TcoFs regulated by their phosphorylation status determines the activity on transcription is frequently used, such as for SRC-3, CDC6, etc. (16, 17).

Although regulation of transcription factors by p38 signaling pathway has been well studied, the interplay of TcoFs with the p38 signaling pathway has not yet been determined. In this study, we report a new mechanism in which hyperphosphorylation of TcoFs directed by constitutive activation of p38 mediates their nuclear export, which cross talks with diverse signaling pathways, including CRE-mediated transcription, AP-1 activation, cell cycle regulation, and protein degradation. In the case of CRTC2 (a TcoF for CREB), we demonstrated that constitutively activated p38 hyperphosphorylated CRTC2 to promote its nuclear export, resulting in shutdown of CRE-mediated transcription, and that this nuclear export was independent of the CRM1-mediated nucleocytoplasmic shuttle process. In addition, we also demonstrated that constitutive activation of p38 hyperphosphorylated transcription factor FOS to drive its nuclear export through CRM1. These results imply that hyperphosphorylation-mediated nuclear export might be a common mechanism to regulate the nucleocytoplasmic transport of cofactors and to promote transcription factor nuclear export as well.

RESULTS

Constitutive activation of p38 inhibits certain transcription factors. We began to study the biological functions of constitutively activated p38 by measuring the time course of p38 activation in HEK293T cells treated with various stimuli. Cells treated with tumor necrosis factor alpha (TNF-α), H_2O_2, or sorbitol exhibited similar dynamic levels of phosphorylated p38 (P-p38), which peaked at early time points ($\sim$10 min) and quickly declined over time (Fig. 1A). In contrast, arsenite treatment induced high and sustained levels of P-p38 (Fig. 1B), indicating constitutive activation of p38. However, activation of NF-κB in arsenite-treated cells was still transient (Fig. 1B), demonstrating differential activation profiles of p38 and NF-κB in arsenite-treated cells. To determine the biological outcome upon constitutive activation of p38, we examined the effects of constitutive activation of p38 on transcription regulation using a set of previously described luciferase reporter-based assays. To selectively activate p38, we coexpressed MKK6(E), a constitutively active form of p38 upstream kinase MKK6, with p38 in HEK293T cells, which led to constitutive p38 activation (Fig. 1C). Constitutive activation of p38 dramatically inhibited luciferase reporter gene expression driven by transcription factors CRE, EGR-1, AP-1, and MTF-1 (Fig. 1D to F and G) but not by NF-κB or interferon (IFN)-stimulated response element (ISRE) (Fig. 1H and I), suggesting differential inhibitory effects of constitutively activated p38 on these transcriptional factors. Thus, constitutive activation of p38 had a negative effect on certain transcription factors.

Constitutive activation of p38 regulates cellular localization of some transcription cofactors. To search for the function of constitutively active p38 in transcription, we constructed a panel of expression plasmids containing 300 transcription cofactors (the TocFs were from the database identified by Schaefer et al. [10]) fused with green fluorescent protein (GFP) and coexpressed each of the plasmids with MKK6(E)/p38 in HEK293T cells. The cells were examined at 24 h posttransfection by confocal laser

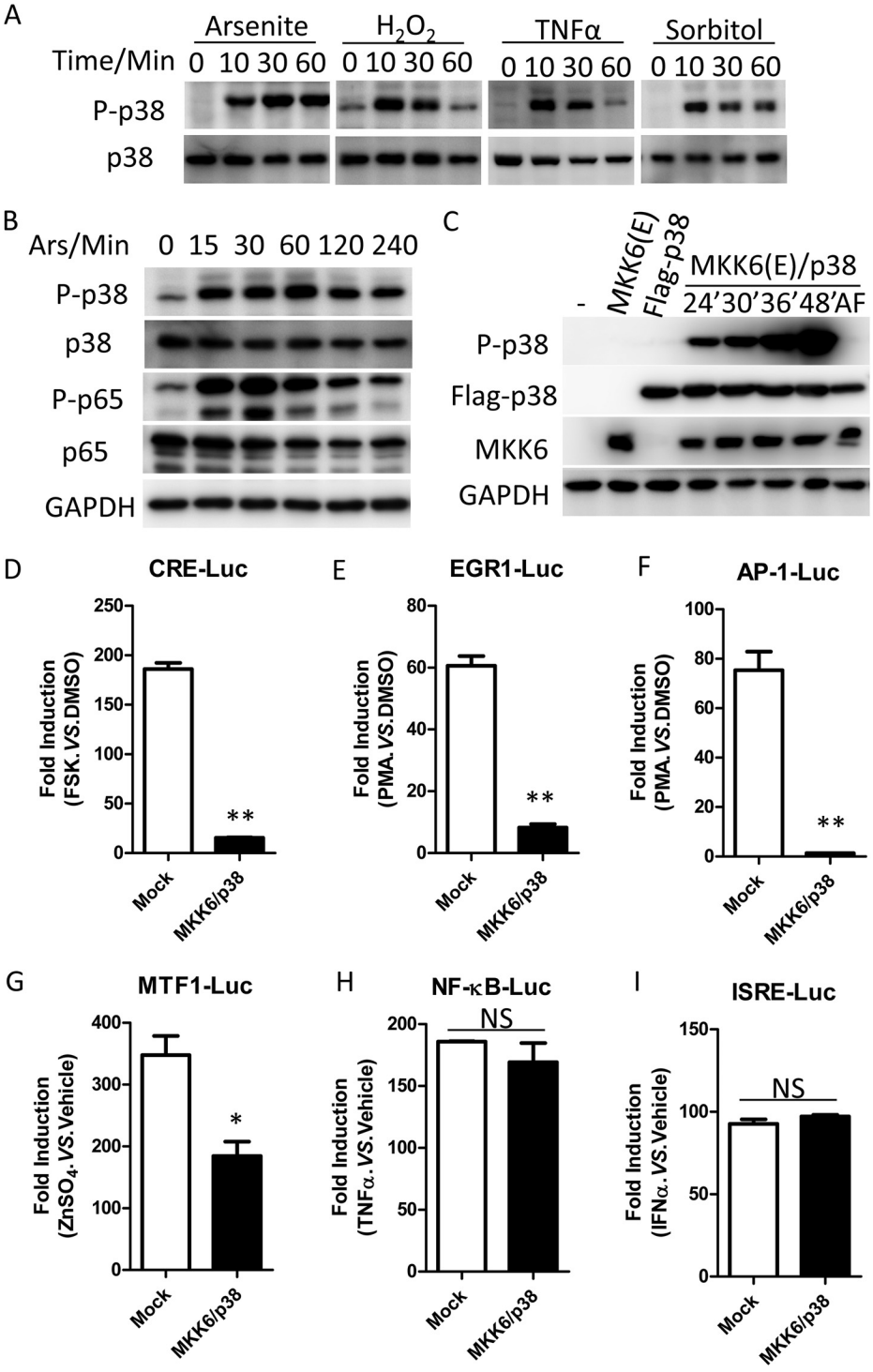

FIG 1 Constitutive or transient activation of p38 results in different biological functions. (A) Western blot of lysates from HEK293T cells treated with various stimuli (1 mM arsenite, 1 mM H_2O_2, 30 ng/ml TNF-α, or 0.2 M sorbitol) for the indicated durations. (B) Western blot of lysates from cells stimulated with 1 mM arsenite for the indicated times (0, 15, 30, 60, 120, and 240 min). (C) Western blot of lysates from cells coexpressing MKK6(E) with p38. Lysates were collected at 24 h, 30 h, 36 h, and 48 h posttransfection. MKK6(E) is a constitutively active form of p38 upstream kinase MKK6. AF is an inactive mutant of p38, p38 T180A/Y182F. (D to I). Luciferase reporter assays of cells coexpressing MKK6(E)/p38 with different transcription factors. For CRE-Luc, transfected cells were stimulated with DMSO or forskolin (FSK) (10 μM) for 4 h; for EGR1-Luc and AP-1-Luc, transfected cells were stimulated with DMSO or PMA (200 nM) or a control for 4 h; for NF-κB-Luc, MTF1-Luc, and ISRE-Luc, transfected cells were stimulated with vehicle, TNF-α (30 ng/ml), $ZnSO_4$ (100 μM), or IFN-α (100 IU/ml) for 4 h. All data represent fold induction compared with the control. The results shown are mean ± SD. **, $P < 0.01$; NS, not significant. These experiments were repeated more than three times.

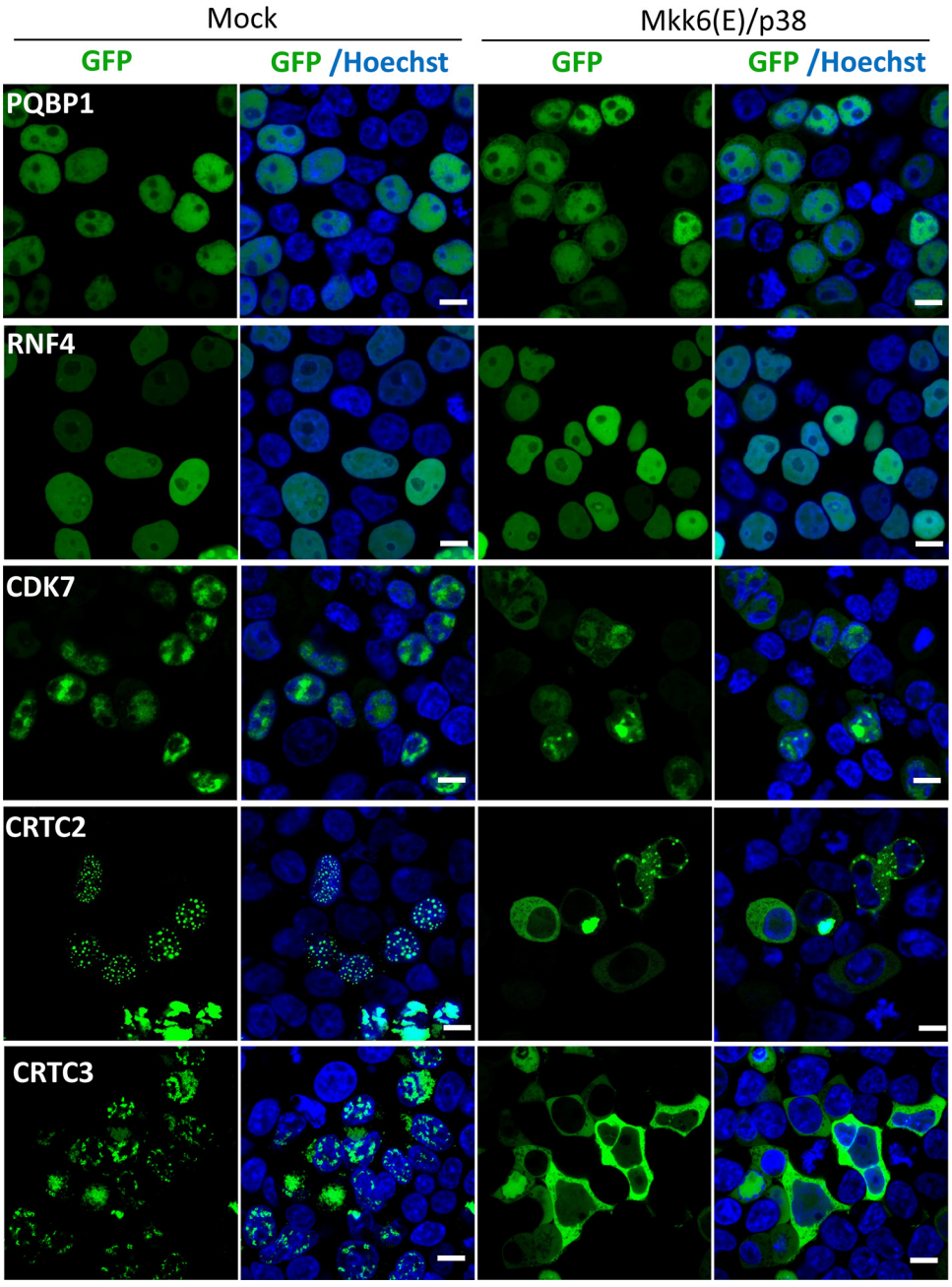

FIG 2 Screening of the cellular localization of TcoFs in MKK6(E)/p38-expressing cells. A library consisting of 300 plasmids expressing GFP-fused TcoFs was used. Individual plasmids were coexpressed by an empty vector or MKK6(E)/p38 in HEK293T cells. At 24 h posttransfection, the cellular localizations of GFP-fused TcoFs were assessed by Leica LSM780 confocal laser scanning microscopy. The nucleus was stained with Hoechst stain. Scale bars, 10 μm.

scanning microscopy. Most of these factors were localized in nucleus regardless of the presence of MKK6(E)/p38, such as PQBP1, RNF4, cyclin-dependent kinase 7 (CDK7), etc. (Fig. 2). Six TcoFs were identified to translocate from nucleus to cytosol in an MKK6(E)/p38-dependent manner (CRTC2 and CRTC3, for example) (Fig. 2). To validate this observation, we analyzed subcellular localization of GFP-CRTC2 in cells expressing MKK6(E) plus wild-type p38 (Flag-p38-WT) or inactive p38 mutant T180A/Y182F (Flag-p38-AF). As shown in Fig. 3A, similar to the case for GFP-CRTC2 alone, the cellular distribution of GFP-CRTC2 was localized mainly in the nucleus in MKK6(E)/p38-AF cells, while coexpression with MKK6(E)/p38-WT mediated relocation of GFP-CRTC2 from

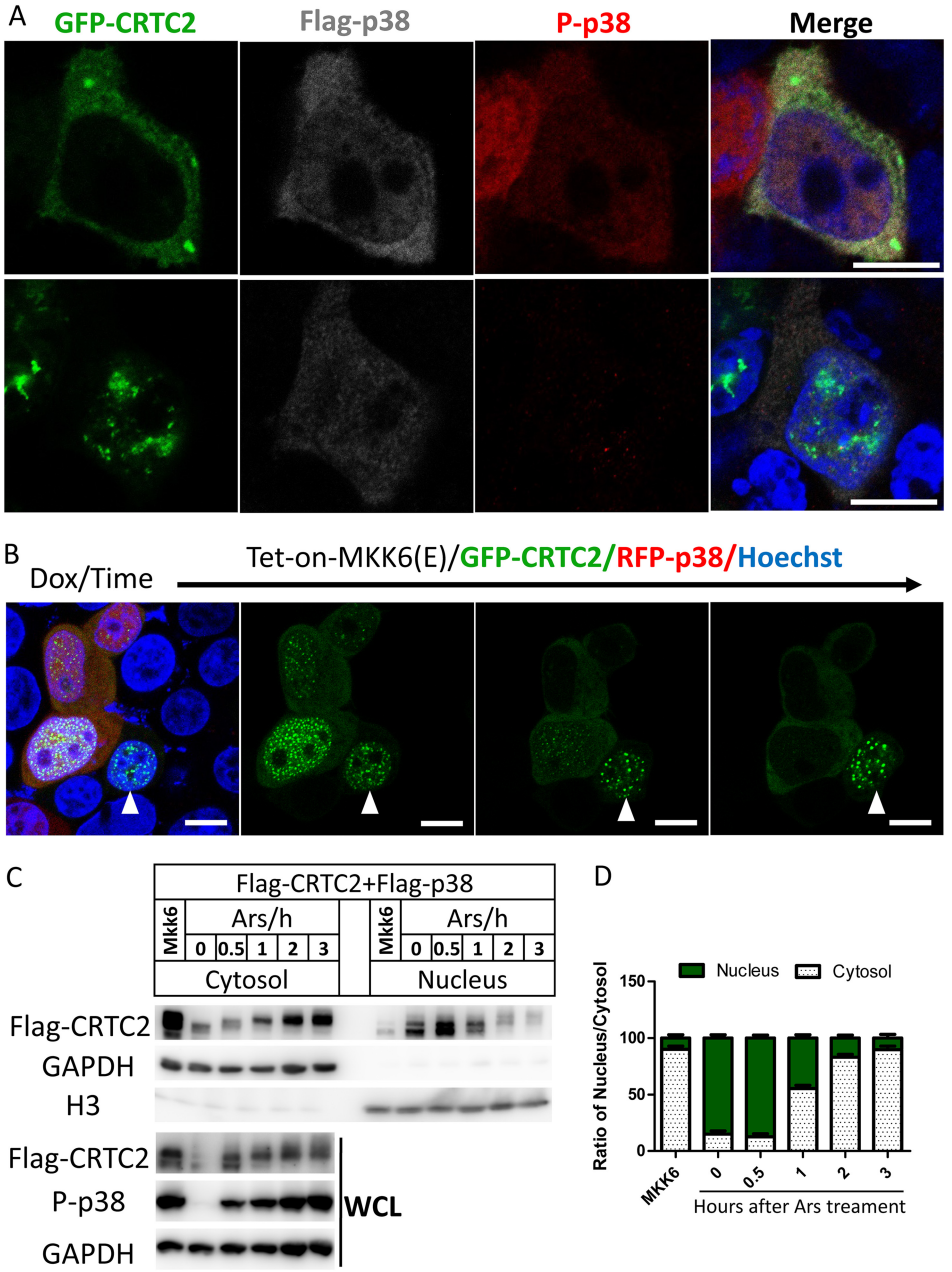

FIG 3 Constitutive activation of p38 drives nucleocytoplasmic transport of CRTC2. (A) Confocal imaging of cells coexpressing GFP-CRTC2 with MKK6(E)/Flag-p38-WT (upper panel) or -AF (lower panel). Cells were assessed at 24 h posttransfection. Flag-p38 and P-p38 were immunostained and observed. The nucleus was stained with Hoechst stain. Scale bars, 10 μm. (B) Live video imaging of the nucleocytoplasmic transport of GFP-CRTC2 in cells expressing doxycycline-inducible MKK6(E). Cells were transfected with GFP-CRTC2 and RFP-p38. Images were acquired every 10 min for 3 h upon doxycycline induction. Scale bars, 20 μm. (C) Western blot of the cytosolic and nuclear fractions of Flag-tagged-CRTC2 (Flag-CRTC2)-expressing cells. Cells coexpressing Flag-CRTC2 and p38 were treated with arsenite for the indicated times. Cotransfection of MKK6 was used as a positive control. Cytosolic and nuclear fractions were isolated using hypotonic buffer. An antibody against GAPDH was used as a cytosol marker. An antibody against histone 3 (H3) was used as a nucleus marker. WCL, whole-cell lysate. (D) Quantification of the cytosolic and nuclear distribution of Flag-CRTC2 shown in panel C. The results are shown as the ratio of nuclear to cytosol distribution. The data shown are representative of three independent experiments.

nucleus to cytosol. The cytosol relocation of CRTC2 is most likely mediated by phosphorylation, and the phosphorylation of CRTC2 by p38 likely occurred in nucleus since CRTC2 was localized mainly in the nucleus and active p38 (P-p38) was also observed in the nucleus. To further confirm this observation, we generated a doxycycline inducible

MKK6(E)-expressing cell line [Tet-on-MKK6(E)], which allows doxycycline to induce constitutive activation of p38 through MKK6(E) expression. We transfected Tet-on-MKK6(E) cells with red fluorescent protein (RFP)-p38 and GFP-CRTC2 expression vectors and observed that GFP-CRTC2 located predominantly in the nucleus and RFP- p38 located in both the nucleus and cytosol in resting cells (Fig. 3B). Upon treatment with doxycycline, GFP-CRTC2 translocated from nucleus to cytosol in RFP-p38-expressing cells but was retained in the nucleus in RFP-p38-negative cells (indicated by arrowheads in Fig. 3B). Consistent with the immunofluorescence results, arsenite-induced translocation of Flag-CRTC2 from nucleus to cytosol was determined by nuclear-cytosolic fractionation assay (Fig. 3C and D). Collectively, these findings demonstrated that constitutive activation of p38 induced by arsenite or coexpressed MKK6(E) drove the nucleocytoplasmic translocation of CRTC2.

Nucleocytoplasmic translocation of CRTC2 driven by constitutive p38 activation shuts down CRE-mediated transcription. We then explored the interplay of constitutive activation-triggered p38 signaling with CRTC2-induced CRE-mediated transcription. Consistent with previous studies (11), overexpression of transcription factor CREB in HEK293T cells exerted little effect on CRE luciferase reporter expression. Treatment with the cAMP activator forskolin (FSK) efficiently induced CRE reporter expression (~50-fold), and overexpression of CRTC2 alone dramatically induced CRE reporter expression (~500-fold) (Fig. 4A). To further study the role of CRTC2 in CRE-mediated transcription in HEK293T cells, we generated CRTC2 knockout cells by the clustered regularly interspaced short palindromic repeat (CRISPR)/Cas9 method. Compared with parental wild-type cells, CRTC2-deficient cells failed to respond to the FSK-induced CRE reporter, indicating that CRTC2 is indispensable for cAMP-induced CRE transcription in HEK293T cells (Fig. 4B).

We next investigated how p38-mediated nucleocytoplasmic transport of CRTC2 affects its coactivity on CRE-mediated transcription. To begin, we generated a cell line with stable expression of CRTC2 plus a CRE reporter (CRTC2+). As shown in Fig. 4C, coexpression of MKK6(E) with p38 dramatically inhibited CRTC2-induced CRE reporter expression, whereas this effect is absent in cells expressing MKK6(E) or p38 alone. Moreover, this effect was dependent on the kinase activity of p38, as loss-of-function p38 mutations (p38-AF and p38-KM, a kinase-dead mutant) or pharmacological inhibition of p38 abolished this effect in CRTC2+ cells (Fig. 4C). To ensure that only constitutive p38 activation suppresses CRE reporter expression, we included stimulation with TNF-α, H_2O_2, or sorbitol in the experiments. We observed that unlike the expression of MKK6(E)/p38 or arsenite treatment, transient activation of p38 by TNF-α, H_2O_2, or sorbitol cannot block CRTC2-induced CRE transcription (Fig. 4D). Notably, no blockade of CRTC2-induced CRE-mediated transcription was observed upon constitutive activation of extracellular signal-regulated kinase (ERK) and Jun N-terminal protein kinase (JNK) (Fig. 4E). We further determined whether this mechanism is conserved in other CRTC family members. Similarly to CRTC2, CRTC1 and CRTC3 dramatically induced CRE-mediated transcription, which was substantially inhibited by MKK6(E)/p38 overexpression (Fig. 4F). Taken together, the results show that constitutive activation of p38 blocks CRE-mediated transcription by regulating the nucleocytoplasmic translocation of CRTCs, indicating that constitutively activated p38 is an effective negative regulator of CRE-mediated transcription.

p38 phosphorylates CRTC2 on multiple sites. To elucidate the molecular mechanism underlying the nucleocytoplasmic translocation of CRTCs driven by constitutive p38 activation, we assessed whether CRTC2 is a direct substrate of p38. The interaction of hemagglutinin (HA)-CRTC2 with Flag-p38 was examined by coimmunoprecipitation (Fig. 5A). The truncation mapping confirmed that CRTC2 strongly interacts with p38 through its N-terminal (amino acids [aa] 1 to 168) and C-terminal (aa 500 to 693) domains (Fig. 5B). We then examined whether CRTC2 was phosphorylated by constitutive activation of p38. SDS-PAGE showed "upshifted" CRTC2 bands induced by MKK6(E)/p38 overexpression and arsenite, and cytosolic CRTC2 had more shifted

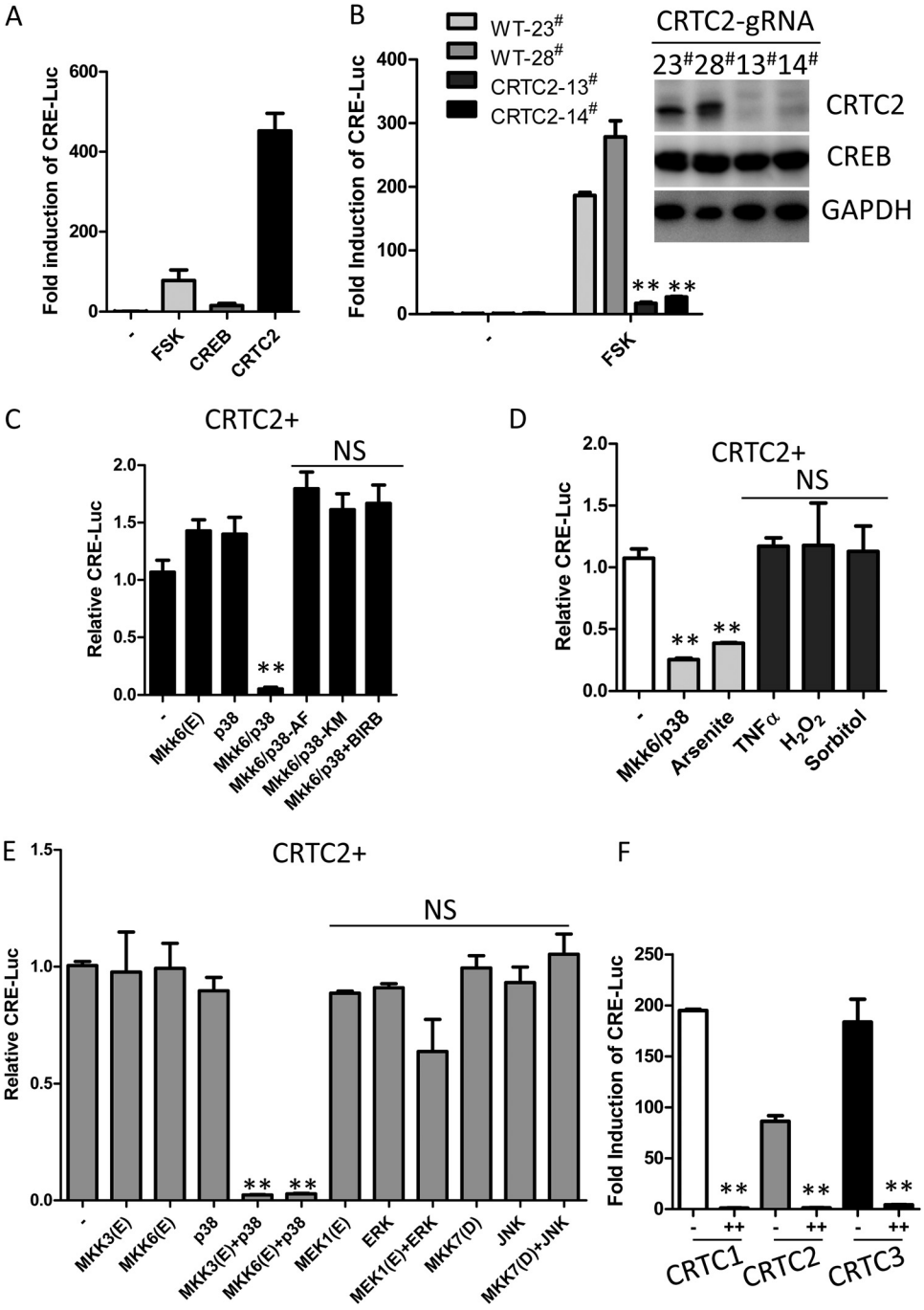

FIG 4 Constitutive activation of p38 inhibits CRE-mediated transcription. (A) Luciferase reporter assay of HEK293T cells cotransfected CRE-Luc with either empty vector, CREB, or CRTC2. Cells were treated with DMSO or FSK (10 μM) for 4 h. (B) Luciferase reporter assay of CRTC2 knockout HEK293T cells transfected with CRE-luciferase reporter and stimulated with DMSO or FSK (10 μM) for 4 h. (C) Luciferase reporter assay of cells stably expressing CRTC2 and CRE-luc (CRTC2+ cells). Cells were transfected with either MKK6(E), p38-WT, MKK6(E)/p38-WT, MKK6(E)/p38-AF(T180A/Y182F), or MKK6(E)/p38-KM(K53M) and treated or not treated with the p38 inhibitor BIRB-796 (BIRB) (10 μM). (D) Luciferase reporter assay of CRTC2+ cells either transfected with MKK6(E)/p38 or treated with 1 mM arsenite, 30 ng/ml TNF-α, 1 mM H_2O_2, or 0.2 M sorbitol for 4 h. (E) Luciferase reporter assay of CRTC2+ cells transfected with either empty vector, MKK3(E), MKK6(E), p38, MKK3(E)/p38, MKK6(E)/p38, MEK1(E), ERK, MEK1(E)/ERK, MKK7(D), JNK, or MKK7(D)/JNK. Cells were lysed at 24 h after transfection. (F) Luciferase reporter assay of cells cotransfected with CRE-Luc and CRTC1, CRTC2, or CRTC3 alone (−) or together with MKK6(E)/p38 (++). Cells were lysed 24 h after. All the data represent fold induction or level relative to that for the control. The results shown are mean ± SD. **, $P < 0.01$; NS, not significant. These experiments were repeated more than three times.

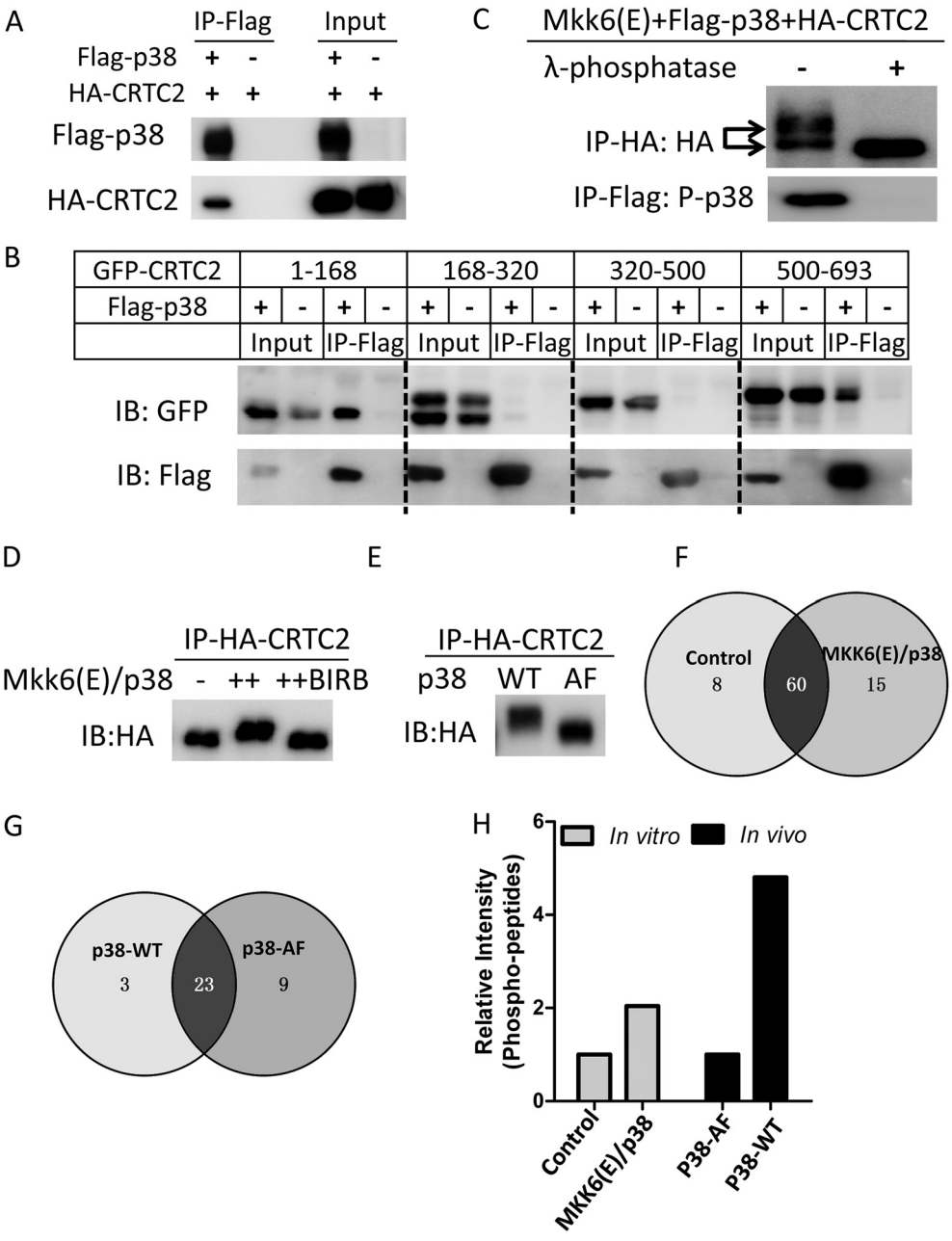

FIG 5 CRTC2 is hyperphosphorylated by p38. (A) Western blot of coimmunoprecipitation of Flag-p38 with HA-tagged-CRTC2 (HA-CRTC2) in HEK293T cells. Coimmunoprecipitation (co-IP) was performed using anti-Flag M2 beads. Antibodies against Flag and HA were used for Western blotting. (B) Western blot of coimmunoprecipitation of Flag-p38 with GFP-tagged-CRTC2 truncates (CRTC2 aa 1 to 168, 168 to 320, 320 to 500, and 500 to 693) in HEK293T cells. Coimmunoprecipitation was performed using anti-Flag M2 beads. Antibodies against Flag and HA were used for Western blotting. (C) *In vitro* dephosphorylation assay of MKK6(E)/p38-phosphorylated CRTC2. HA-CRTC2 was purified from cells coexpressing MKK6(E)/Flag-p38 using anti-HA beads and incubated with λ-phosphatase. Purified Flag-p38 was used as a positive control. Antibodies against Flag and HA were used for Western blotting. (D) *In vitro* kinase assay for HA-CRTC2. HA-CRTC2 purified from overexpression in HEK293T cells was incubated with recombinant MKK6(E) and p38 in the absence of the p38 inhibitor BIRB-796 (10 μM). Antibodies against Flag and HA were used for Western blotting. (E) *In vivo* phosphorylation of HA-CRTC2 in HEK293T cells. Cells were cotransfected with HA-CRTC2 and MKK6(E)/p38-WT or MKK6(E)/p38-AF. HA-CRTC2 was purified from cells coexpressing MKK6(E)/Flag-p38 using anti-HA beads. An antibody against HA was used for Western blotting. (F) Venn diagram of the phosphorylation sites of CRTC2 identified by LC-MS/MS assay from the experiment shown in panel D. Detailed sites are shown in Table 1. (G) Venn diagram of the phosphorylation sites of CRTC2 identified by LC-MS/MS assay from the experiment shown in panel E. Detailed sites are shown in Table 2. (H) Quantification of the intensity of phosphopeptides obtained for panels F and G.

TABLE 1 Detailed phosphorylation sites of CRTC2 obtained from MS *in vitro*, related to Fig. 5F

CRTC2-HA incubation	Phosphorylation sites
Control	T3, S4, S11, S23, T37, S49, T50, S65, S70, S79, S86, S90, S116, S127, S128, S136, S141, S142, S164, S171, S173, S178, S183, T279, S308, S320, S346, S348, S355, S357, S358, S366, S368, S376, T385, S386, S391, S393, S398, S400, S403, S404, S405, S408, S419, S424, S433, S436, S447, S456, T458, S460, S464, S465, S475, S478, S490, S492, T497, T501, S504, S512, S516, S519, S579, S613, S624, S628
With MKK6(e)/p38	T3, S4, S11, S23, T37, S70, S79, S90, S116, S127, S131, S136, S141, S142, S164, S173, T177, S178, S183, T279, S300, S320, S336, S339, S342, S346, S348, S355, S357, S358, S366, S368, S376, T384, T385, S386, S391, S393, S398, S400, S403, S404, S405, S407, S408, S415, S419, S424, S433, S436, S447, S456, T458, S460, T462, S464, S465, T467, S478, S489, S490, S492, T497, T501, S504, S512, S514, S516, S519, S579, T599, S613, S624, S628, S644

proteins (Fig. 3C). To determine whether these "upshifted" bands were the consequence of phosphorylation, we performed an *in vitro* dephosphorylation assay using λ-phosphatase. As shown in Fig. 5C, treatment with λ-phosphatase increased the rate of migration of CRTC2 from MKK6(E)/p38-expressing cells, showing that constitutive activation of p38 induced the phosphorylation status of CRTC2. To further probe whether CRTC2 is a direct substrate of p38, *in vitro* kinase assays were performed using recombinant MKK6(E) and p38. Figure 5D shows purified CRTC2 with "upshifted" bands upon incubation with recombinant MKK6(E) and p38, which was reversed by adding the p38 inhibitor BIRB-796. Taken together, these data indicated that p38 interacted directly with and phosphorylated CRTC2.

To identify the phosphorylation sites of CRTC2 mediated by p38, CRTC2 phosphorylated *in vivo* and *in vitro* was purified separately and then analyzed by liquid chromatography-tandem mass spectrometry (LC-MS/MS). For the *in vivo* assay, HA-CRTC2 was coexpressed with MKK6(E)/p38-WT or with MKK6(E)/p38-AF (control) in HEK293T cells and then immunoprecipitated with anti-HA beads (Fig. 5E). For the *in vitro* assay, HA-CRTC2 purified from HEK293T cells overexpressing it was incubated with or without recombinant MKK6(E) plus p38 (Fig. 5D). The proteins immunoprecipitated from *in vivo* and kinase assay reactions were resolved by SDS-PAGE, the bands corresponding to CRTC2 were further cut from the gel and then digested by trypsin, and the phosphopeptides were enriched by immobilized metal ion affinity chromatography and then analyzed by LC-MS/MS. The *in vitro* kinase assay resulted in 75 phosphorylation sites in the MKK6(E)/p38 group and 68 sites in the control, whereas the *in vivo* assay yielded 26 phosphorylation sites in MKK6(E)/p38-WT-expressing cells and 32 sites in MKK6(E)/p38-AF-expressing cells (Fig. 5F and G). The numbers of p38-dependent phosphorylation sites identified in the *in vivo* and *in vitro* assays were 15 and 3, respectively. Quantitative MS data revealed that the intensities of CRTC2 phosphopeptides in MKK6(E)/p38-WT samples were much higher than those in MKK6(E)/p38-AF or control samples (Fig. 5H), raising the possibility that p38 phosphorylates CRTC2 on multiple sites simultaneously.

To understand the role of phosphorylation sites in regulating CRTC2 function, we generated a series of non-phospho-CRTC2 A mutants (with serine/threonine-to-alanine mutations) carrying single mutations of all potential residues and tested their capacity to induce the CRE-mediated transcription in the presence of constitutively activated p38. Akin to the case for wild-type CRTC2, MKK6(E)/p38 overexpression efficiently blocked all the CRE-mediated transcription induced by all the CRTC2 A mutants (Fig. 6A). Consistently, the cellular localization of these A mutants exhibited the same pattern as wild-type CRTC2 (data not shown). Because constitutive activation of p38 led

TABLE 2 Detailed phosphorylation sites of CRTC2 obtained from MS *in vivo*, related to Fig. 5G

Protein cotransfected	Phosphorylation sites
MKK6(E)/p38-WT	S23, S70, S79, S86, S90, S116, S128, S134, S136, S164, S183, T192, S236, S237, S239, S433, S436, S447, S490, S492, S497, T501, S613, S620, S623, S624
MKK6(E)/p38-AF	S70, S79, S86, S90, S116, S127, S128, S131, S134, S136, S164, S178, S183, T192, S236, S237, S433, S436, S447, S456, S478, S489, S490, S492, S497, T501, S520, S613, S620, S623, S624, S686

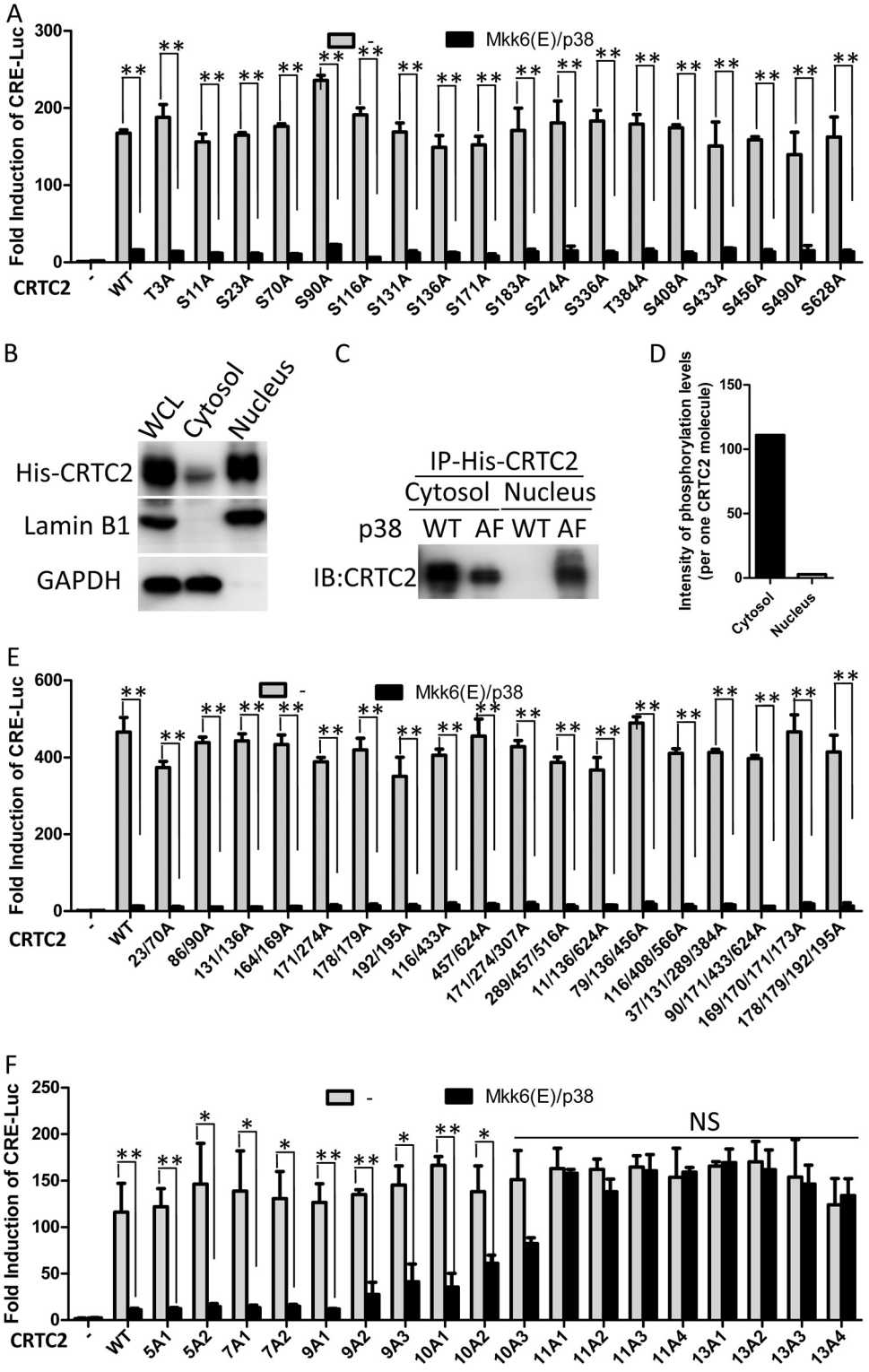

FIG 6 p38 phosphorylates CRTC2 at multiple sites, which inhibits its activity for CRE-mediated transcription. (A) CRE-luciferase reporter assay of cells expressing different non-phospho-CRTC2 mutants. HEK293T cells were cotransfected with different non-phospho-CRTC2 mutants with empty vector or MKK6(E)/p38. Cells were lysed at 24 h after transfection and subjected to luciferase reporter assay. (B) Western blot of the nuclear and cytosolic fractions from cells expressing 6×His-CRTC2. An antibody against GAPDH was used as a cytosol marker. An antibody against lamin B1 was used as a nuclear marker. WCL, whole-cell lysate. (C) Western blot of the pulldowns of 6×His-CRTC2 from the nuclear and cytosolic fractions under denaturing condition. Cells were cotransfected with 6×His-CRTC2, MKK6(E) and p38-WT, or MKK6(E) and p38-AF. The nuclear and cytosolic fractions were isolated using hypotonic buffer. 6×His-CRTC2 was pulled down from these fractions using Ni-NTA spin columns under denaturing

(Continued on next page)

TABLE 3 Detailed mutation sites of CRTC2, related to Fig. 6F

Mutant	Sites mutated to A
5A1	S131/S171/S274/S433/S624
5A2	T37/S116/T289/S456/S613
7A1	S70/S79/S86/S90/S306/T307/S308
7A2	T177/S178/T192/S195/S306/T307/S308
9A1	S170/S171/S173/T177/S178/S183/S306/T307/S308
9A2	T37/S116/S171/S173/T177/S178/T289/S456/S613
9A3	S70/S79/S86/S90/S306/T307/S529/S623/S624
10A1	T37/S116/S171/S173/T177/S178/S274/T289/S456/S613
10A2	T177/S178/T192/S195/S306/T307/S308/S464/S465/S529
10A3	S131/S170/S171/T196/S255/T296/S306/T307/S308
11A1	S70/S79/S86/S90/S127/S128/S131/S136/S456/T458/S460
11A2	T3/S11/S70/S90/S116/S131/S136/S171/S183/S274/S336
11A3	S11/S70/S79/S86/S90/S306/T307/S308/S433/S456/S490
11A4	T177/S178/T192/S195/306/T307/S308/T620/S623/S624/S628
13A1	S70/S79/S86/S90/S306/T307/S308/S609/S613/T620/S623/S624/S628
13A2	S70/S79/S86/S90/S127/S128/S131/S136/S456/T458/S460/S623/S624
13A3	T177/S178/T192/S195/306/T307/S308/S609/S613/T620/S623/S624/S628
13A4	T3/S11/S70/S90/S116/S131/S136/S171/S183/S274/S336/T384/S456

to a high intensity of phosphorylation of CRTC2, we proposed that nuclear export of CRTC2 requires a certain level of hyperphosphorylation (Fig. 5H). To verify this hypothesis, CRTC2 in the cytosolic and nuclear fractions was purified, and absolute phosphopeptide intensities were quantified using mass spectrometry with a spiked-in heavy-amino-acid-labeled peptide. As the nuclear fractions failed to dissolve well in normal immunoprecipitation buffer (1% Triton X-100 or 1% NP-40), His-CRTC2 was used in this assay. The nuclear and cytosol fractions were dissociated as usual, and then His-CRTC2 was pulled down with Ni-nitrilotriacetic acid (NTA) spin columns in denaturing buffer (8 M urea). Akin to the case for Flag or GFP-CRTC2, the nuclear and cytosol distribution of His-CRTC2 in the p38-WT group was different from those in the inactive p38-AF group and the no-p38 group. Like the no-p38 group, the p38-AF group cannot drive CRTC2 cytosolic translocation (Fig. 6B and C). Absolute quantification of phosphopeptide intensities revealed that the phosphorylation level of cytosolic translocated CRTC2 was more than 10-fold higher than that of nuclear CRTC2 (Fig. 6D). The hyperphosphorylation of CRTC2 is likely to be essential for CRTC2 cytosolic localization.

To explore the precise sites responsible for cytosolic relocation of CRTC2, we generated a series of non-phospho-CRTC2 mutants carrying combinational assortments of different sites and then determined their subcellular localizations and capacity for induction of CRE-mediated transcription. Mutants carrying fewer than 5 mutations of identified sites (CRTC2-2A, -3A, and -4A) showed activity in MKK6(E)/p38-overexpressing cells that was similar to that of wild-type CRTC2 (Fig. 6E). However, mutants with 9 or more mutations showed increasing resistance to MKK6(E)/p38 overexpression-induced inhibition of CRE-mediated transcription, of which mutants carrying $\geq$11 (CRTC2-11A) mutations were completely resistant to MKK6(E)/p38 overexpression-mediated inhibition (Fig. 6F). Consistently, CRTC2 mutants with $\geq$11 A mutations retained nuclear localization in MKK6(E)/p38-overexpressing cells (Fig. 7A

FIG 6 Legend (Continued)
condition (8 M urea). An antibody against CRTC2 was used for Western blotting. (D) Quantitative MS analysis of phosphorylation levels per CRTC2 molecule of cytosolic and nuclear CRTC2 purified for panel C. (E) CRE-luciferase reporter assay of cells expressing different non-phospho-CRTC2 mutants (2A, 3A, and 4A mutants). HEK293T cells were cotransfected with different non-phospho-CRTC2 mutants with empty vector or MKK6(E)/p38. Cells were lysed at 24 h after transfection and subjected to luciferase reporter assay. (F) CRE-luciferase reporter assay of cells expressing randomly generated 5A, 7A, 9A, 10A, 11A, and 13A mutants of CRTC2 (detailed mutation sites are shown in Table 3). HEK293T cells were cotransfected with different non-phospho-CRTC2 mutants with empty vector or MKK6(E)/p38. Cells were lysed at 24 h after transfection and subjected to luciferase reporter assay. All of the luciferase data represent fold induction compared to the control. The results shown are mean $\pm$ SD. *, $P < 0.05$; **, $P < 0.01$; NS, not significant. These experiment were repeated more than three times.

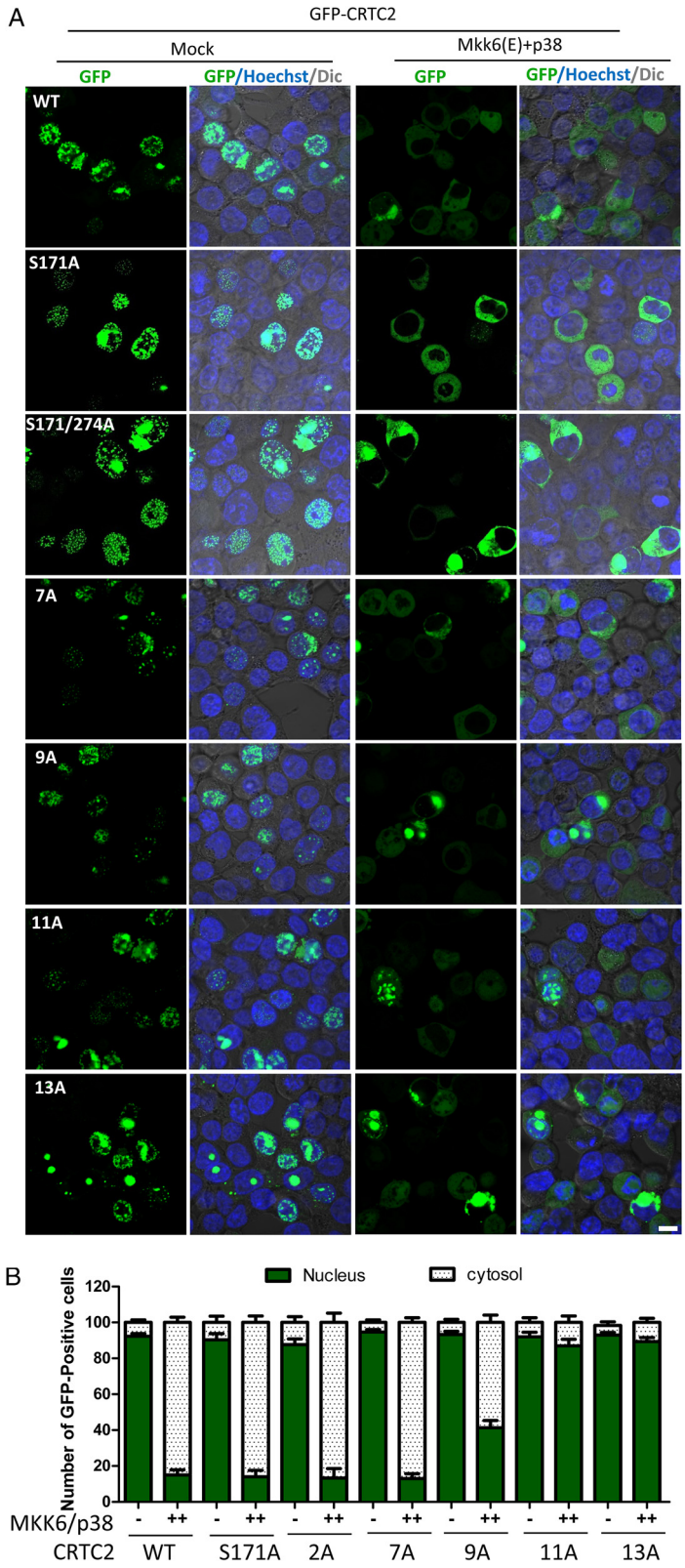

FIG 7 Hyperphosphorylation promotes the nucleocytoplasmic transport of GFP-CRTC2. (A) Confocal imaging of cells expressing GFP-CRTC2 WT or nonphosphorylated mutants. HEK293T cells were cotransfected with GFP-CRTC2 WT or nonphosphorylated mutants with empty vector (−) or with MKK6(E) plus p38 (++) and imaged at 24 h posttransfection. The nucleus was stained with Hoechst stain. Scale bar, 10 μm. (B) Quantification of panel A. One hundred GFP-positive cells were quantified under each condition. The data shown are representative of three independent experiments.

and B). These results indicated that hyperphosphorylation of CRTC2 on multiple (≥11) sites by constitutively active p38 is responsible for cytosolic relocation of CRTC2 and subsequent blockade of CRE-mediated transcription.

CRM1-independent cytosolic relocation of CRTC2 driven by constitutively activated p38. Nucleocytoplasmic transport requires export transporter and RanGTP (18). The export of about 90% of proteins from the nucleus to the cytosol is dependent on the nuclear export sequence (NES) sensor CRM1 (19). After recognition of NES-containing proteins, CRM1 cooperatively binds to RanGTP, forming a trimeric transport complex which is subsequently transported from nucleus to cytosol through the nuclear pore complexes (NPCs) (20–22). It had been predicted that CRTC2 contained two nuclear export sequences (NES1 and NES2) within the region of amino acids 145 to 320. As constitutive activation of p38 drives cytosolic translocation of CRTC2 via hyperphosphorylation, we assessed whether this hyperphosphorylation-mediated nucleocytoplasmic transport is dependent on the NES-CRM1 exporting system. Surprisingly, a CRTC2 mutant lacking NES (with deletion of aa 145 to 320) showed a cytosolic location similar to that of wild-type CRTC2 in MKK6(E)/p38-overexpressing cells (Fig. 8A). In addition, leptomycin B (LMB), a specific inhibitor of nuclear export that binds to CRM1, did not affect MKK6(E)/p38-induced cytosol relocation of CRTC2 (Fig. 8B). However, LMB treatment led to an increase of nuclear p38 and P-p38 and decrease of cytosolic p38 and P-p38 (Fig. 8B). The fact that reduction of cytosolic P-p38 did not affect CRTC2 nuclear export supports the notion that phosphorylation of CRTC2 is mediated by nuclear p38. Consistent with these results, removal of NES or treatment with LMB failed to reverse the inhibition of CRE-mediated transcription by constitutive activation of p38 (Fig. 8C). Collectively, our data indicate that constitutive p38 activation-induced cytosol relocation of CRTC2 is through an undocumented nuclear exporting mechanism.

Constitutive activation of p38 regulates cytosolic translocation of transcription factor FOS through hyperphosphorylation. Since hyperphosphorylation on random sites in CRTC2 regulated its subcellular localization, we asked whether this is a common mechanism. As inhibition mediated by MKK6(E)/p38 on phorbol myristate acetate (PMA)-induced AP-1–luciferase activity was also observed (Fig. 1E) and the AP-1 component FOS was reported as the substrate of p38 (23), we investigated whether this hyperphosphorylation-driven nucleocytosolic transport model is applicable to FOS. Similar to the investigation of CRTC2, GFP-FOS was coexpressed with MKK6(E) in the presence of p38-WT or p38-AF in HEK293T cells. As expected, the cellular localization of GFP-FOS was mostly at the nucleus in MKK6(E)/p38-AF-expressing cells. Interestingly, ~30% of the GFP-FOS was exported to the cytosol in MKK6(E)/p38-WT-expressing cells (Fig. 9A and C). In contrast to what we observed for CRTC2, pretreatment with LMB blocked the cytosol translocation of GFP-FOS in MKK6(E)/p38-WT-expressing cells (Fig. 9B and C). These results indicate that MKK6(E)/p38 promoted GFP-FOS translocation to the cytosol through a CRM1-exporting system.

We then investigated whether hyperphosphorylation is involved in MKK6(E)/p38-promoted nucleocytoplasmic transport of GFP-FOS. Based on reported data, there are four phosphorylation sites in FOS (Thr-232, Thr-325, Thr-331, and Ser-374). We generated a 4A mutant (T232/T325/T331/S374A) but found that it could be exported to cytosol like wild-type FOS when MKK6(E)/p38 was coexpressed (Fig. 9D). Since a database search revealed other phosphorylation sites in FOS, we generated more A mutants of FOS, as we did in studying CRTC2, and then coexpressed these A mutants with MKK6(E)/p38 in HEK293T cells. MKK6(E)/38 coexpression had no effect on nuclear export of a 2A/3A/4A mutant; however, A mutations on ≥5 potential phosphorylation sites blocked MKK6(E)/p38-mediated cytosol translocation of FOS (Fig. 9D). Taken together, these results indicate that hyperphosphorylation is potentially a common mechanism to drive cytosolic export of nuclear proteins.

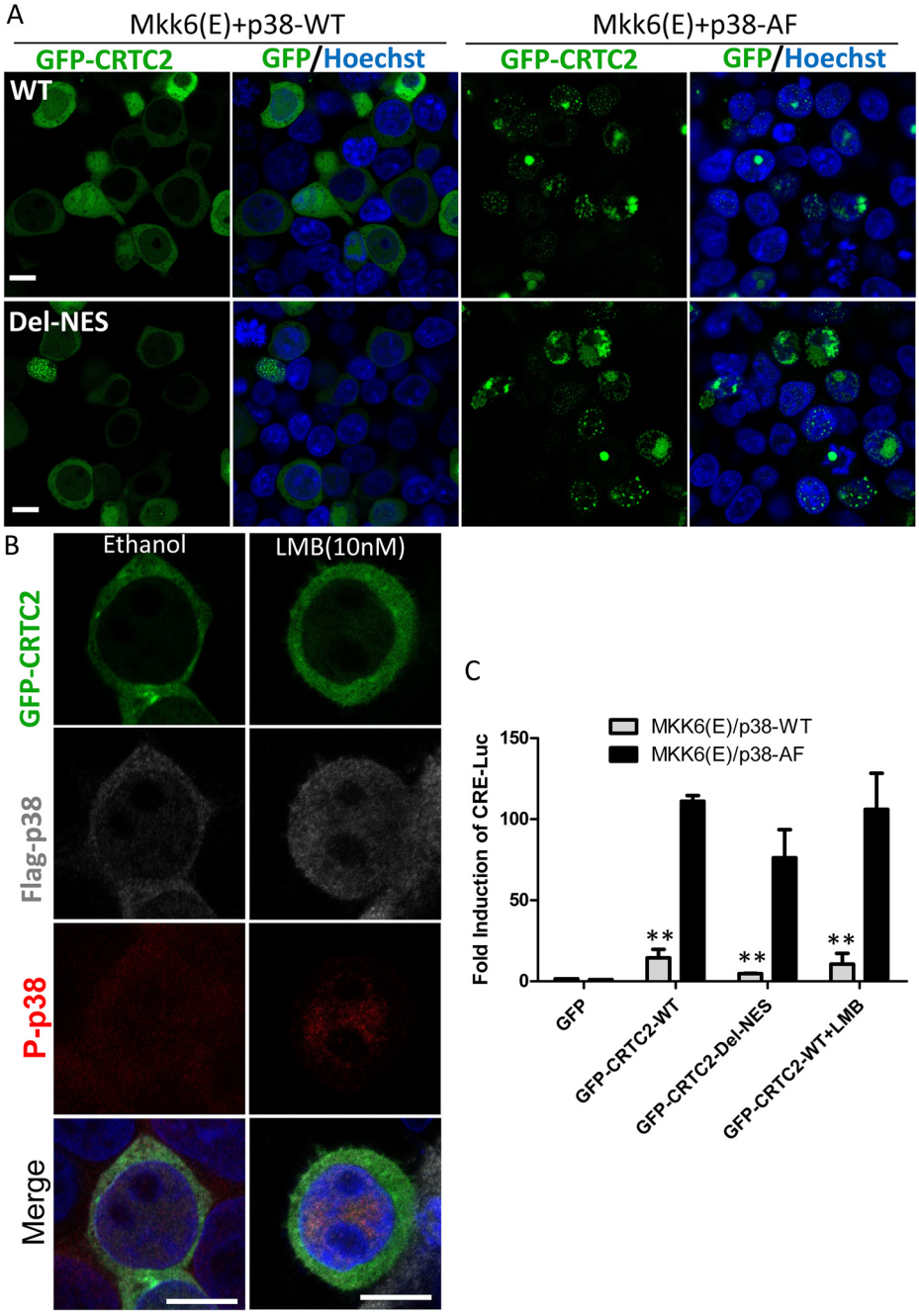

FIG 8 p38 drives CRTC2 nuclear export independently of CRM1. (A) Confocal imaging of HEK293T cells expressing CRTC2 WT and a CRTC2 mutant lacking the NES (aa 145 to 320). Cells were cotransfected with CRTC2 WT or a CRTC2 mutant lacking the NES (aa 145 to 320) and MKK6(E)/p38-WT or MKK6(E)/p38-AF. (B) Confocal imaging of GFP-CRTC2-expressing HEK293T cells. Cells were cotransfected with GFP-CRTC2 and MKK6(E)/p38 and treated with 10 nM LMB or ethanol as the vehicle control at 12 h after transfection. Cells were assessed by confocal microscopy at 24 h after transfection. Flag-p38 and P-p38 were immunostained and observed. Scale bars, 10 μm. (C) CRE-luciferase assay of cells expressing CRTC2 WT, CRTC2 NES-mutant treated or not treated with LMB. Cells were cotransfected with GFP-CRTC2 WT or the GFP-CRTC2 NES mutant with MKK6(E)/p38-WT or MKK6(E)/p38-AF and treated with LMB at 12 h after transfection. Cells were lysed and subjected to luciferase assay at 24 h posttransfection. All of the luciferase data represent fold induction compared to the control. The results shown are mean ± SD. **, $P < 0.01$; NS, not significant. These experiment were repeated more than three times.

DISCUSSION

p38 is a master regulator and transducer of myriad intracellular signaling pathways during gene expression. Prior research has focused largely on the role of p38 in positive regulation of transcription factors, including ATF1, -2, and -6, SRF accessory protein

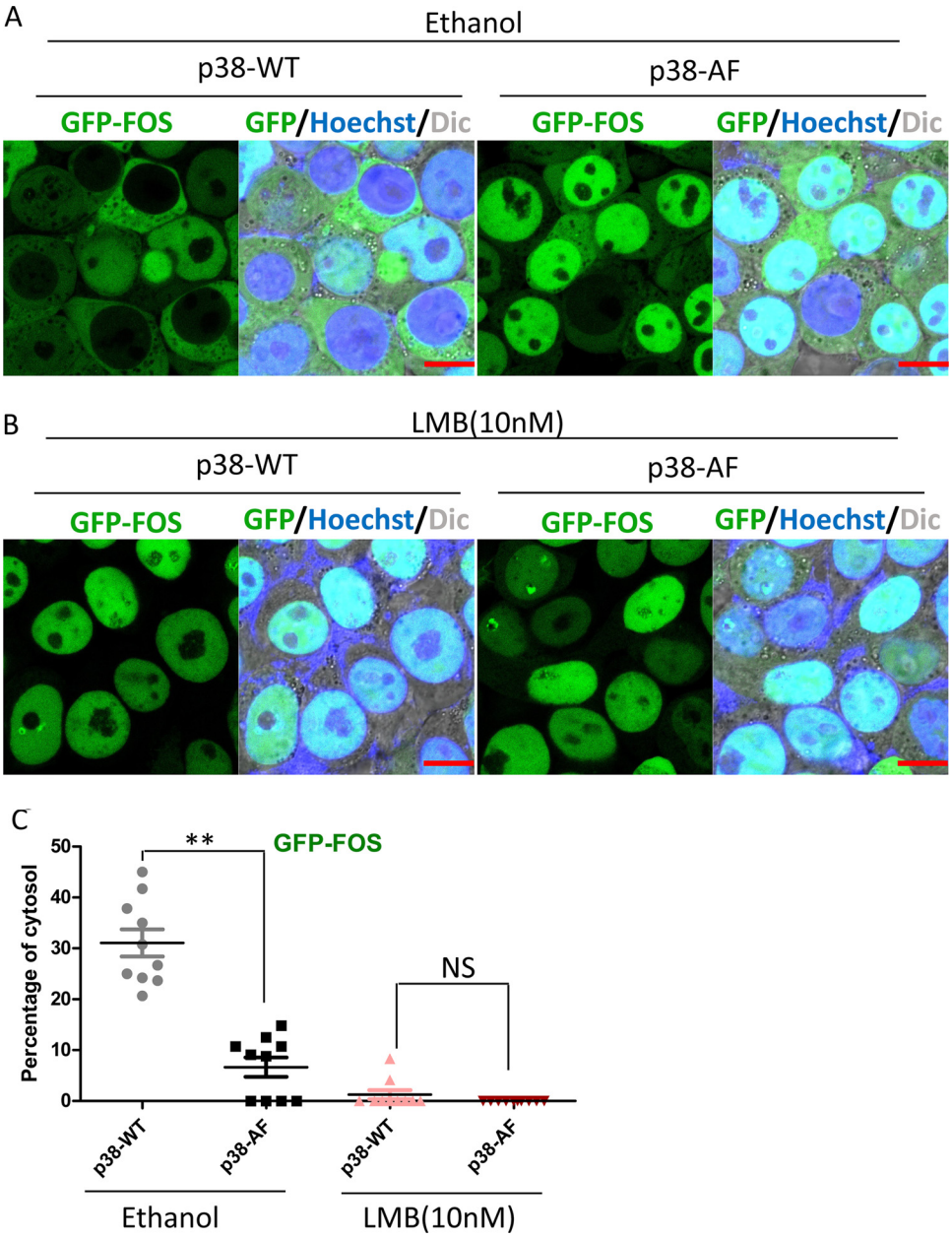

FIG 9 MKK6(E)-p38 regulates cytosolic translocation of FOS by hyperphosphorylation. (A and B) Confocal imaging of HEK293T cells expressing GFP-tagged FOS (GFP-FOS). Cells stably expressing GFP-FOS were transfected with MKK6(E)/p38-WT or MKK6(E)/p38-AF and treated with 10 nM LMB at 12 h after transfection. Cells were assessed by confocal microscopy at 24 h after transfection. The nucleus was stained with Hoechst stain. Scale bars, 20 μm. (C) Quantification of panels A and B. Ten fields containing 100 GFP-positive cells were quantified under each condition. The results shown are mean $\pm$ SD. **, $P < 0.01$; NS, not significant. This experiment was performed more than three times. (D) Confocal imaging of HEK293T cells expressing GFP-FOS mutants (4A, 6A, 9A, and 12A mutants; detailed mutation sites are shown in Table 4). Cells were cotransfected with GFP-FOS mutants with empty vector or MKK6(E)/p38 and assessed at 24 h after transfection by confocal microscopy. The nucleus was stained with Hoechst stain. Scale bars, 10 μm.

(Sap1), CHOP (growth arrest and DNA damage inducible gene 153, or GADD153), p53, C/EBPβ, myocyte enhancing factor 2C (MEF2C), MEF2A, Usf-1, DDIT3, ELK1, and NFAT (6, 24–33). Here we uncovered a hitherto-unexpected function of p38 to negatively regulate gene expression, whereby constitutively activated p38 hyperphosphorylated CRTC2, resulting in its nucleocytoplasmic transport and sequential shutdown of CRE-mediated transcription.

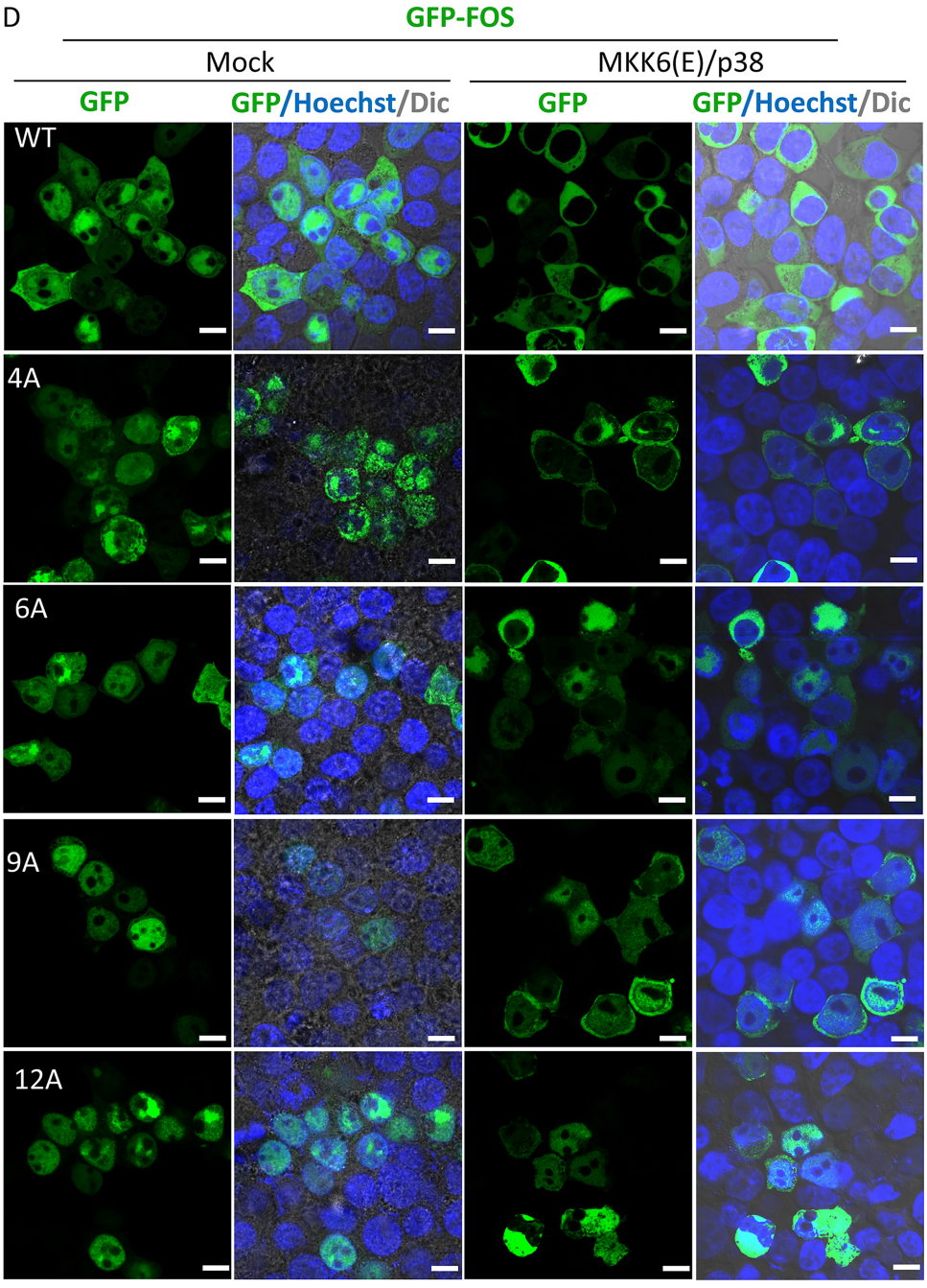

FIG 9 (Continued)

In eukaryotic cells, basic life activities such as the replication and transcription of genes occur in the nucleus, while the translation and modification of protein take place in the cytoplasm. Consequently, thousands of macromolecules are shuttling between the nuclear and cytosolic compartments through the nuclear pore complex (NPC)

TABLE 4 Detailed mutation sites of FOS, related to Fig. 9D

Mutant	Sites mutated to A
4A	T232/T325/T331/S374
6A	S4/S68/T69/S277/S278/S374
9A	S4/T51/S68/T69/S133/T162/S177/S277/S278
12A	S4/T51/S68/T69/S133/T162/S177/S277/S278/T325/T331/S374

(34–37). Nucleocytoplasmic shuttling is extremely complicated and tightly regulated. Many proteins spatially shuttle between the nucleus and cytoplasm in response to cell cycle progression, growth signals, or environmental stimuli (38, 39). Phosphorylation status-mediated nucleocytoplasmic shuttling of CRTC2 has been reported (13, 14). Under basal condition, CRTC2 is phosphorylated on serine 171 by the salt-inducible kinases (SIKs) and sequestered in the cytoplasm through interaction with 14-3-3 proteins, while cAMP and calcium signals promote the dephosphorylation of CRTC2 through inhibition of SIKs and activation of the phosphatase calcineurin (CN), respectively, which leads to its nucleotranslocation. We made the CRTC2 S171A mutant, which was confined in nucleus and induced robust CRE-mediated transcription under basal conditions, confirming the critical role of S171 phosphorylation in CRTC2 trafficking as documented in prior studies. Unexpectedly, we identified the relocation of CRTC2 S171A from the nucleus to the cytosol, enabled by constitutively activated p38 and blockade of its activity on inducing CRE-mediated transcription (Fig. 6A and 7A). In addition, both deletion of NES and pharmacological inhibition of CRM1 failed to block the nucleocytoplasmic transport of CRTC2 mediated by constitutive activation of p38 (Fig. 8A and B). Taken together, these findings indicate an alternative mechanism of regulating CRE-mediated transcription by constitutive activation of p38 signaling.

Phosphorylation on multiple amino acid residues of a protein is often tightly regulated in biological processes (40). The accumulative role of phosphorylation at multiple sites has been shown to regulate protein subcellular localization (41, 42). It has also been reported that phosphorylation at multiple sites controls the affinity of a cargo for its transport receptor. For instance, the transcription factor Pho4 is phosphorylated by the CDK-cyclin complex Pho85-Pho80 on 5 serine residues, dictating its subcellular localization by promoting the association with export receptor and decreasing the affinity for import receptor, resulting in its rapid nuclear export (43–45). Due to technical difficulties in analyzing hyperphosphorylated proteins, ectopic expression of genes was often used, and we did so in our study of CRTC2 phosphorylation. We believe that the data obtained in our experiments could closely mimic the endogenous situation, as we had detected p38-dependent S624 phosphorylation of endogenous CTRC2 by MS analysis. Because p38 can activate certain kinases and some of the phosphorylation sites in CRTC2 are not typical p38 phosphorylation sites, the possibility that another kinase(s) also participates in the hyperphosphorylation of CRTC2 cannot be excluded.

In this study, we uncovered that, in contrast to the functionality of single or multiple defined sites, the phosphorylation of CRTC2 on a series of randomly occurring serine or threonine residues mediated its nucleocytoplasmic transport, which we have termed the "hyperphosphorylation-driven nuclear export model." In other words, a series of serine or threonine residues need to be randomly phosphorylated to reach a certain threshold to exert nuclear export. Random phosphorylation may be linked to the adoption of a flexible or unfolded conformation by the target protein, so that several residues become equally accessible to the kinase. Additionally, this hyperphosphorylation-driven nuclear export mechanism can also be applied to the transcription factor FOS.

The regulation of the p38 signaling transduction pathway is cellular context dependent. Our results indicated that hyperphosphorylation of cofactors or transcription factors by constitutively activated p38 might represent a new mechanism to regulate the nucleocytoplasmic transport of these factors and further to suppress their function. Although the physiological processes in which this mechanism may play a role await further investigation, constitutive activation of p38 has been found in a number of situations, such as in various malignant tumors. It was reported that the constitutive activation of p38 inhibited osteoblastogenesis and bone formation in myeloma-bearing SCID mice, resulting in bone destruction (46). Our previous data also showed that enforced activation of p38 by MKK6(E) restored MyoD function and enhanced MEF2 activity in rhabdomyosarcoma, leading to growth arrest and terminal differentiation (47). Additionally, deletion of the p38-specific dual-specificity phosphatases (DUSP1 to

-4) also promoted activity of unrestrained p38, resulting in cardiomyopathy and increased mortality with aging (48). It is possible that hyperphosphorylation-mediated nuclear export of CRTC2 participates in the physiological processes in which constitutive activation of p38 occurs.

MATERIALS AND METHODS

Plasmid constructs and gene expression. The constructs pcDNA3-Flag-p38-WT/AF/KM, ERK, JNK, no-tag MKK3/6(E), MEK1(E), and MKK7(D) used here were generated previously in our lab (6, 49, 50). The transcriptional response element (TRE) sequences cloned into the pGL3-vector are referred to as reporter genes (Promega): CRE, GCACCAGACAGTGACGTCAGCTGCCAGATCCCATGGCCGTCATACTGTGACGTCTTTC AGACACCCCATTGACGTCAATGGGAGAACAGAT; EGFR1, CGCCCCCGC(6×); AP-1, TGACTAA(7×); MTF1, GAGCTCTGCACTCCGCCC(5×); NF-κB, GGGGACTTTCC(6×); ISRE, TAGTTTCACTTTCCC(6×). CRTC2 was amplified from human cDNA and cloned into pBOB or pLV-puromycin lentivirus vector with no tag or with N-terminally tagged Flag, HA, or 6×His by the exonuclease III (Exo III)-assisted ligase-free cloning method. The cDNAs of human transcription cofactors described here were PCR amplified from our reverse-transcribed cDNA library. Full-length cDNAs of cofactors were cloned into the pBOB-N-GFP vector using the Exo III-assisted ligase-free cloning method. Deletion mutants and all of the A mutants of CRTC2 and FOS were introduced using standard PCR or two rounds of PCR.

Antibodies and reagents. The following antibodies were obtained from Cell Signaling: p38/p-p38, ERK/p-ERK, JNK/p-JNK, and p65/p-p65. Mouse anti-glyceraldehyde-3-phosphate dehydrogenase (anti-GAPDH) (60004-1-Ig) and lamin B1(66095-1-Ig) were purchased from Proteintech, mouse anti-GFP was purchased from Abmart, monoclonal anti-Flag M2 antibody produced in mouse (F3165) was obtained from Sigma, anti-TORC2 (454-607) rabbit antibody was obtained from EMD Millipore, CREB1 polyclonal antibody (A1189) was purchased from Abclonal, and mouse anti-HA (F-7)was obtained from Santa Cruz Biotechnology, Inc. (Santa Cruz, CA). Lambda protein phosphatase (P0753S) was obtained from NEB. Arsenite, H_2O_2, sorbitol, PMA, forskolin, $ZnSO_4$, and doxycycline were purchased from Sigma, human TNF was obtained from eBioscience (San Diego, CA), and human interferon alpha A (Alpha 2a) was purchased from PBL Assay Science.

Cell culture and transfection. HEK293T cells were purchased from ATCC. Stable expression of the CRTC2-plus-CRE reporter cell line (CRTC2+), the GFP-FOS cell line, and the Tet-on-MKK6(E) cell line was generated by adding 2 μg/ml puromycin for selection at 48 h posttransfection. The CRTC2 knockout HEK293T cells were generated using the CRISPR/Cas9 technology (51, 52), and the targeting sequence was 5′-GAACGGGCCTGGTTCGGCCA-3′. All the cells were cultured in Dulbecco's modified Eagle's medium (DMEM) supplemented with 10% fetal bovine serum, 2 mM L-glutamine, 100 IU penicillin, and 100 mg/ml streptomycin and were kept at 37°C in a humidified atmosphere containing 5% CO_2.

HEK293T cells were transfected by the calcium phosphate precipitation method after overnight incubation. The transfection medium was changed 12 h later, and cells were kept in culture for the following analysis.

Luciferase assays. HEK293T cells were seeded in a 24-well plate containing culture medium as described above. After overnight incubation, cells were transfected with the indicated expression constructs using the calcium phosphate transfection method. A control reporter construct containing *Renilla* luciferase (Rluc) (pRL-TK) was cotransfected for normalization of transfection efficiency. At 48 h posttransfection, cells were washed with phosphate-buffered saline (PBS) and lysed with passive lysis buffer (Promega). The culture plates were placed on a rocking platform for 15 min at room temperature. Finally, the dual luciferase activities were determined with the Promega dual-luciferase reporter kit (E1980) and GloMax20/20 single-tube luminometer (Promega Corporation) following the manufacturer's instruction (Promega). Firefly luciferase activities were normalized to *Renilla* luciferase reporter activities and are shown as fold induction compared with the control. The results shown are the averages from duplicate or triplicate determinations, with error bars representing standard deviations (SD). All experiments were independently replicated at least two or three times.

Confocal microscopy. For fixed-cell imaging, cells were first washed with PBS and then fixed with freshly prepared 4% paraformaldehyde (PFA) in PBS for 15 min. The fixed cells were then permeabilized in 0.2% Triton X-100 in PBS, blocked with 3% bovine serum albumin in PBS, stained with rabbit anti-Flag (1:200; Sigma) and mouse anti-P-p38 (1:100; Cell Signaling Technology), and labeled with goat anti-rabbit IgG(H+L) highly cross-adsorbed secondary antibody (Alexa Fluor 647; Invitrogen) or goat anti-mouse IgG(H+L) cross-adsorbed secondary antibody (Alexa Fluor 568; Invitrogen). Finally, the cells were counterstained with Hoechst stain to visualize the nuclei. All images were captured and processed using identical settings in a Zeiss LSM 780 laser scanning confocal microscope with a 100×/1.49 numerical aperture (NA) oil objective.

For live-cell imaging, Tet-on-MKK6(E) cells were seeded in 35-mm glass-bottom dishes (Nest, Shanghai, China). Time-lapse images were acquired every 15 min for several hours, depending on the nuclear export process, after transfection by the calcium phosphate precipitation method at about 36 h. GFP was excited under a 488-nm argon laser, and RFP was excited under a 568-nm argon laser. Nuclei were stained using Hoechst 33342 stain (1:10,000) and excited under a 405-nm argon laser. Imaging was carried out using the Zeiss LSM 780 with a 100×/1.49 NA oil objective in a 37°C incubator containing 5% CO_2.

Nucleus and cytosol disassociation. HEK293T cells were seeded in 35-mm dishes at 24 h post-transfection with the indicated expression constructs, treated with arsenite at the indicated times, and washed with 1 ml PBS, and then 800 μl nuclear extraction buffer (0.01 M Tris-HCl, 0.01 M NaCl, 0.003 M

$MgCl_2$, 0.03 M sucrose, and 0.5% NP-40) was added to scrape the cells (35-mm dish). The cells were then transferred to a 1.5-ml Eppendorf (EP) tube, and the tube was put on a rotor at 4°C for 10 min. The cell lysate was centrifuged further at 1,500 × *g* at 4°C for 10 min to obtain the cytosolic fraction. The supernatant (about 600 μl) was transferred to another 1.5-ml EP tube (with 120 μl 5× SDS sample buffer) and taken as cytosol. The remaining supernatant was discarded, the pellet was washed with 1 ml nuclear extraction buffer and spun, and the supernatant was removed. The pellet was washed 3 times, and finally 400 μl 1.2× SDS was added to the pellet to obtain the nuclear fraction.

Immunoprecipitation and Western blotting. HEK293T cells were seeded in 6-well plates and transfected as indicated for 36 h. Cells were lysed with 400 μl lysis buffer (20 mM Tris-HCl [pH 7.5], 150 mM NaCl, 1 mM EGTA, 1 mM Na_2EDTA, 1% Triton X-100, 2.5 mM sodium pyrophosphate, 1 mM β-glycerophosphate, 1 mM Na_3VO_4) per well after one PBS wash. The plate was placed on ice for 30 min, 20 μl 2× SDS sample buffer was added to 20 μl cell lysate in a new 1.5-ml EP tube as the total cell lysate, and the residual cell lysate (380 μl) was centrifuged at 20,000 × *g* for 30 min. The supernatant was immunoprecipitated with anti-Flag M2 beads or anti-HA beads as indicated at 4°C overnight. After immunoprecipitation, the beads were washed three times in 500 μl lysis buffer. The supernatant was discarded, and the beads were subsequently eluted with SDS sample buffer. Western blot analysis of cell lysates and immunoprecipitates using anti-Flag, anti-GFP, anti-CRTC2, and other antibodies was performed as indicated.

***In vitro* dephosphorylation assay.** HA-CRTC2, MKK6(E), and Flag-p38 were coexpressed in HEK293T cells. At 24 h posttransfection, HA-CRTC2 and Flag-p38 were immunoprecipitated with anti-HA beads or anti-Flag M2 beads separately, and then the immunoprecipitates were washed three times with phosphatase buffer (50 mM HEPES [pH 7.5], 100 mM NaCl, 2 mM dithiothreitol, 0.01% Brij 35, 1 mM $MnCl_2$) and divided into two parts. One was augmented with 200 units of λ-phosphatase (NEB), and the other was mock treated. After incubation at 30°C for 30 min with gentle shaking, the reactions were stopped by the addition of 5× SDS sample buffer followed by boiling for 5 min, and then Western blot analysis of anti-HA or P-p38 was performed.

***In vitro* kinase assay.** HA-CRTC2 was purified from HEK293T cells by immunoprecipitation with anti-HA beads, and then the immunoprecipitates were washed 3 times with kinase buffer (25 mM Tris [pH 7.5], 10 mM $MgCl_2$, 2 mM dithiothreitol [DTT], 5 mM β-glycerophosphate, 0.1mM Na_3VO_4). The beads were suspended in 30 μl of kinase buffer (plus 10 mM ATP) and then incubated with recombinant MKK6(E) and p38 at 30°C for 30 min with gentle shaking. The reactions were stopped by the addition of 5× SDS sample buffer followed by boiling for 5 min, and then Western blot analysis or mass spectrometric analysis was performed.

MS analysis. The phosphorylated CRTC2 proteins from *in vivo* coexpression or *in vitro* kinase assay were subjected to SDS-PAGE. The bands responding to CRTC2 proteins were excised and subjected to in-gel digestion. Briefly, the gels were cut into 1-mm^3 cubes and destained with 50 mM NH_4HCO_3–50% acetonitrile. The proteins were reduced using 25 mM DTT–50 mM NH_4HCO_3 at 56°C for 20 min, and cysteines were alkylated using 5 mM iodoacetamide–50 mM NH_4HCO_3 for 20 min at room temperature in the dark. After adding 200 ng trypsin, digestions were performed at 37°C overnight. The peptides were desalted with zip tips, followed by immobilized-metal affinity chromatography (IMAC)–Fe^{3+} enrichment as previously described (53). Peptides were dissolved in 50 μl 1% acetic acid–60% acetonitrile, incubated with 5 μl IMAC beads, and shaken for 30 min at room temperature. After the IMAC beads were washed with 50 μl 1% acetic acid–60% acetonitrile twice, phosphopeptides were eluted with 5% $NH_3.H_2O$. For absolute quantification of phosphorylation levels of CRTC2, we purchased the synthetic peptide CRTC2 GGILDGEMDPK, which contained a heavy-amino-acid-labeled K (^{13}C-6, ^{15}N-2). Phosphopeptides were analyzed on a TripleTOF 5600 (AB Sciex) mass spectrometer (MS) coupled to a NanoLC Ultra 2D Plus (Eksigent) high-pressure liquid chromatography (HPLC) system. Peptides were first bound to a 5-mm by 500-μm trap column packed with Zorbax C_{18} 5-μm, 200-Å resin using 0.1% (vol/vol) formic acid–2% acetonitrile in H_2O at 10 μl/min for 5 min and then separated using a 60-min gradient from 2 to 35% buffer B (buffer A is 0.1% [vol/vol] formic acid and 5% dimethyl sulfoxide [DMSO] in H_2O, and buffer B is 0.1% [vol/vol] formic acid and 5% DMSO in acetonitrile) on a 15-cm by 75-μm in-house pulled emitter-integrated column packed with Magic C_{18} AQ 3-μm, 200-Å resin. The acquired wiff files were searched with Maxquant version 1.5 against the full nonredundant, canonical human genome as annotated by UniProtKB/Swiss-Prot (downloaded in September 2014). The database search parameters were set as follows: carbamidomethylation (C) was set as fixed modification, methionine oxidation and phosphorylation on STY were set as variable modification, and semitryptic peptides and peptides with up to two missed cleavages were allowed. All identified phosphopeptides of CRTC2 proteins were selected and manually checked. For absolute quantitation of phosphopeptides, the amount of the endogenous CRTC2 peptide GGILDGEMDPK was calculated with that of spiked-in heavy-amino-acid-labeled peptide. Subsequently, the amounts of phosphopeptides were calculated by their intensities relative to that of the light peptide GGILDGEMDPK. All of these phosphorylation residues of CRTC2 identified from MS were analyzed in A-mutant assays as follows: $T_3/S_4/S_{11}/S_{23}/T_{37}/S_{70}/S_{79}/\mathbf{S_{86}P}/\mathbf{S_{90}P}/S_{94}/S_{95}/\mathbf{S_{116}P}/S_{127}/\mathbf{S_{128}P}/\mathbf{S_{131}P}/\mathbf{S_{136}P}/S_{170}/S_{171}/T_{177}/S_{178}/\mathbf{S_{183}P}/\mathbf{T_{192}P}/S_{195}/\mathbf{S_{255}P}/S_{274}/\mathbf{T_{289}P}/T_{296}/S_{306}/T_{307}/S_{308}/\mathbf{S_{336}P}/\mathbf{S_{358}P}/S_{368}/S_{371}/T_{384}/\mathbf{S_{408}P}/\mathbf{S_{424}P}/\mathbf{S_{433}P}/\mathbf{S_{456}P}/T_{458}/\mathbf{S_{460}P}/S_{464}/S_{465}/\mathbf{S_{490}P}/S_{516}/S_{529}/\mathbf{S_{566}P}/S_{609}/S_{613}/T_{620}/S_{623}/\mathbf{S_{624}P}/S_{628}/S_{644}$, where the consensus p38 phosphorylation sites (Ser/Thr-Pro) are in bold.

Statistical analysis. Statistical analysis was performed with Prism software (GraphPad Software). Data are expressed as mean ± standard deviation (SD). The two-tailed Student *t* test was used to compare differences between treated groups and their paired controls.

ACKNOWLEDGMENTS

We thank Lu Zhou (Xiamen University) for critical reading of the manuscript. We thank Wei Han (Xiamen University) for providing cDNAs of cofactors.

This work was supported by the National Natural Science Foundation of China (81788101), the National Basic Research Program of China (973 Program 2015CB553800), the National Natural Science Foundation of China (31420103910, 81630042, 81700596, and 31500737), the 111 Project (B12001), and the National Science Foundation of China for Fostering Talents in Basic Research (J1310027). This project was also funded by China Postdoctoral Science Foundation (2017M622069) for Huabin Ma.

We declare no competing financial interests.

REFERENCES

1. Ono K, Han J. 2000. The p38 signal transduction pathway: activation and function. Cell Signal 12:1–13. https://doi.org/10.1016/S0898-6568(99)00071-6.
2. Cuadrado A, Nebreda AR. 2010. Mechanisms and functions of p38 MAPK signalling. Biochem J 429:403–417. https://doi.org/10.1042/BJ20100323.
3. Kang YJ, Seit-Nebi A, Davis RJ, Han J. 2006. Multiple activation mechanisms of p38alpha mitogen-activated protein kinase. J Biol Chem 281:26225–26234. https://doi.org/10.1074/jbc.M606800200.
4. Remy G, Risco AM, Iñesta-Vaquera FA, González-Terán B, Sabio G, Davis RJ, Cuenda A. 2010. Differential activation of p38MAPK isoforms by MKK6 and MKK3. Cell Signal 22:660–667. https://doi.org/10.1016/j.cellsig.2009.11.020.
5. Lambert SA, Jolma A, Campitelli LF, Das PK, Yin Y, Albu M, Chen X, Taipale J, Hughes TR, Weirauch MT. 2018. The human transcription factors. Cell 172:650–665. https://doi.org/10.1016/j.cell.2018.01.029.
6. Zarubin T, Han J. 2005. Activation and signaling of the p38 MAP kinase pathway. Cell Res 15:11–18. https://doi.org/10.1038/sj.cr.7290257.
7. Trempolec N, Dave-Coll N, Nebreda AR. 2013. SnapShot: p38 MAPK substrates. Cell 152:924–924.e1. https://doi.org/10.1016/j.cell.2013.01.047.
8. Spiegelman BM, Heinrich R. 2004. Biological control through regulated transcriptional coactivators. Cell 119:157–167. https://doi.org/10.1016/j.cell.2004.09.037.
9. Rosenfeld MG, Lunyak VV, Glass CK. 2006. Sensors and signals: a coactivator/corepressor/epigenetic code for integrating signal-dependent programs of transcriptional response. Genes Dev 20:1405–1428. https://doi.org/10.1101/gad.1424806.
10. Schaefer U, Schmeier S, Bajic VB. 2011. TcoF-DB: dragon database for human transcription co-factors and transcription factor interacting proteins. Nucleic Acids Res 39:D106–D110. https://doi.org/10.1093/nar/gkq945.
11. Conkright MD, Canettieri G, Screaton R, Guzman E, Miraglia L, Hogenesch JB, Montminy M. 2003. TORCs: transducers of regulated CREB activity. Mol Cell 12:413–423. https://doi.org/10.1016/j.molcel.2003.08.013.
12. Iourgenko V, Zhang W, Mickanin C, Daly I, Jiang C, Hexham JM, Orth AP, Miraglia L, Meltzer J, Garza D, Chirn GW, McWhinnie E, Cohen D, Skelton J, Terry R, Yu Y, Bodian D, Buxton FP, Zhu J, Song C, Labow MA. 2003. Identification of a family of cAMP response element-binding protein coactivators by genome-scale functional analysis in mammalian cells. Proc Natl Acad Sci U S A 100:12147–12152. https://doi.org/10.1073/pnas.1932773100.
13. Altarejos JY, Montminy M. 2011. CREB and the CRTC co-activators: sensors for hormonal and metabolic signals. Nat Rev Mol Cell Biol 12:141–151. https://doi.org/10.1038/nrm3072.
14. Screaton RA, Conkright MD, Katoh Y, Best JL, Canettieri G, Jeffries S, Guzman E, Niessen S, Yates JR, III, Takemori H, Okamoto M, Montminy M. 2004. The CREB coactivator TORC2 functions as a calcium- and cAMP-sensitive coincidence detector. Cell 119:61–74. https://doi.org/10.1016/j.cell.2004.09.015.
15. Luo Q, Viste K, Urday-Zaa JC, Senthil Kumar G, Tsai WW, Talai A, Mayo KE, Montminy M, Radhakrishnan I. 2012. Mechanism of CREB recognition and coactivation by the CREB-regulated transcriptional coactivator CRTC2. Proc Natl Acad Sci U S A 109:20865–20870. https://doi.org/10.1073/pnas.1219028109.
16. Amazit L, Pasini L, Szafran AT, Berno V, Wu RC, Mielke M, Jones ED, Mancini MG, Hinojos CA, O'Malley BW, Mancini MA. 2007. Regulation of SRC-3 intercompartmental dynamics by estrogen receptor and phosphorylation. Mol Cell Biol 27:6913–6932. https://doi.org/10.1128/MCB.01695-06.
17. Petersen BO, Lukas J, Sorensen CS, Bartek J, Helin K. 1999. Phosphorylation of mammalian CDC6 by cyclin A/CDK2 regulates its subcellular localization. EMBO J 18:396–410. https://doi.org/10.1093/emboj/18.2.396.
18. Guttler T, Gorlich D. 2011. Ran-dependent nuclear export mediators: a structural perspective. EMBO J 30:3457–3474. https://doi.org/10.1038/emboj.2011.287.
19. Fornerod M, Ohno M, Yoshida M, Mattaj IW. 1997. CRM1 is an export receptor for leucine-rich nuclear export signals. Cell 90:1051–1060. https://doi.org/10.1016/S0092-8674(00)80371-2.
20. Knockenhauer KE, Schwartz TU. 2016. The nuclear pore complex as a flexible and dynamic gate. Cell 164:1162–1171. https://doi.org/10.1016/j.cell.2016.01.034.
21. Hutten S, Kehlenbach RH. 2007. CRM1-mediated nuclear export: to the pore and beyond. Trends Cell Biol 17:193–201. https://doi.org/10.1016/j.tcb.2007.02.003.
22. Pemberton LF, Paschal BM. 2005. Mechanisms of receptor-mediated nuclear import and nuclear export. Traffic 6:187–198. https://doi.org/10.1111/j.1600-0854.2005.00270.x.
23. Tanos T, Marinissen MJ, Leskow FC, Hochbaum D, Martinetto H, Gutkind JS, Coso OA. 2005. Phosphorylation of c-Fos by members of the p38 MAPK family. Role in the AP-1 response to UV light. J Biol Chem 280:18842–18852. https://doi.org/10.1074/jbc.M500620200.
24. Raingeaud J, Gupta S, Rogers JS, Dickens M, Han J, Ulevitch RJ, Davis RJ. 1995. Pro-inflammatory cytokines and environmental stress cause p38 mitogen-activated protein kinase activation by dual phosphorylation on tyrosine and threonine. J Biol Chem 270:7420–7426. https://doi.org/10.1074/jbc.270.13.7420.
25. Tan Y, Rouse J, Zhang A, Cariati S, Cohen P, Comb MJ. 1996. FGF and stress regulate CREB and ATF-1 via a pathway involving p38 MAP kinase and MAPKAP kinase-2. EMBO J 15:4629–4642. https://doi.org/10.1002/j.1460-2075.1996.tb00840.x.
26. Hazzalin CA, Cano E, Cuenda A, Barratt MJ, Cohen P, Mahadevan LC. 1996. p38/RK is essential for stress-induced nuclear responses: JNK/SAPKs and c-Jun/ATF-2 phosphorylation are insufficient. Curr Biol 6:1028–1031. https://doi.org/10.1016/S0960-9822(02)00649-8.
27. Janknecht R, Hunter T. 1997. Convergence of MAP kinase pathways on the ternary complex factor Sap-1a. EMBO J 16:1620–1627. https://doi.org/10.1093/emboj/16.7.1620.
28. Wang XZ, Ron D. 1996. Stress-induced phosphorylation and activation of the transcription factor CHOP (GADD153) by p38 MAP kinase. Science 272:1347–1349. https://doi.org/10.1126/science.272.5266.1347.
29. Han J, Jiang Y, Li Z, Kravchenko VV, Ulevitch RJ. 1997. Activation of the transcription factor MEF2C by the MAP kinase p38 in inflammation. Nature 386:296–299. https://doi.org/10.1038/386296a0.
30. Huang C, Ma WY, Maxiner A, Sun Y, Dong Z. 1999. p38 kinase mediates UV-induced phosphorylation of p53 protein at serine 389. J Biol Chem 274:12229–12235. https://doi.org/10.1074/jbc.274.18.12229.
31. Galibert MD, Carreira S, Goding CR. 2001. The Usf-1 transcription factor is a novel target for the stress-responsive p38 kinase and mediates UV-induced tyrosinase expression. EMBO J 20:5022–5031. https://doi.org/10.1093/emboj/20.17.5022.

32. Pereira RC, Delany AM, Canalis E. 2004. CCAAT/enhancer binding protein homologous protein (DDIT3) induces osteoblastic cell differentiation. Endocrinology 145:1952–1960. https://doi.org/10.1210/en.2003-0868.
33. Gómez del Arco P, Martínez-Martínez S, Maldonado JL, Ortega-Pérez I, Redondo JM. 2000. A role for the p38 MAP kinase pathway in the nuclear shuttling of NFATp. J Biol Chem 275:13872–13878. https://doi.org/10.1074/jbc.275.18.13872.
34. Cook A, Bono F, Jinek M, Conti E. 2007. Structural biology of nucleocytoplasmic transport. Annu Rev Biochem 76:647–671. https://doi.org/10.1146/annurev.biochem.76.052705.161529.
35. Christie M, Chang CW, Rona G, Smith KM, Stewart AG, Takeda AA, Fontes MR, Stewart M, Vertessy BG, Forwood JK, Kobe B. 2016. Structural biology and regulation of protein import into the nucleus. J Mol Biol 428:2060–2090. https://doi.org/10.1016/j.jmb.2015.10.023.
36. Tetenbaum-Novatt J, Rout MP. 2010. The mechanism of nucleocytoplasmic transport through the nuclear pore complex. Cold Spring Harbor Symp Quant Biol 75:567–584. https://doi.org/10.1101/sqb.2010.75.033.
37. Sloan KE, Gleizes PE, Bohnsack MT. 2016. Nucleocytoplasmic transport of RNAs and RNA-protein complexes. J Mol Biol 428:2040–2059. https://doi.org/10.1016/j.jmb.2015.09.023.
38. Bayliss R, Corbett AH, Stewart M. 2000. The molecular mechanism of transport of macromolecules through nuclear pore complexes. Traffic 1:448–456. https://doi.org/10.1034/j.1600-0854.2000.010602.x.
39. Floch AG, Palancade B, Doye V. 2014. Fifty years of nuclear pores and nucleocytoplasmic transport studies: multiple tools revealing complex rules. Methods Cell Biol 122:1–40. https://doi.org/10.1016/B978-0-12-417160-2.00001-1.
40. Ubersax JA, Ferrell JE. Jr, 2007. Mechanisms of specificity in protein phosphorylation. Nat Rev Mol Cell Biol 8:530–541. https://doi.org/10.1038/nrm2203.
41. Bauer NC, Doetsch PW, Corbett AH. 2015. Mechanisms regulating protein localization. Traffic 16:1039–1061. https://doi.org/10.1111/tra.12310.
42. Salazar C, Hofer T. 2009. Multisite protein phosphorylation–from molecular mechanisms to kinetic models. FEBS J 276:3177–3198. https://doi.org/10.1111/j.1742-4658.2009.07027.x.
43. O'Neill EM, Kaffman A, Jolly ER, O'Shea EK. 1996. Regulation of PHO4 nuclear localization by the PHO80-PHO85 cyclin-CDK complex. Science 271:209–212. https://doi.org/10.1126/science.271.5246.209.
44. Jeffery DA, Springer M, King DS, O'Shea EK. 2001. Multi-site phosphorylation of Pho4 by the cyclin-CDK Pho80-Pho85 is semi-processive with site preference. J Mol Biol 306:997–1010. https://doi.org/10.1006/jmbi.2000.4417.
45. Kaffman A, Rank NM, O'Shea EK. 1998. Phosphorylation regulates association of the transcription factor Pho4 with its import receptor Pse1/Kap121. Genes Dev 12:2673–2683. https://doi.org/10.1101/gad.12.17.2673.
46. Yang J, He J, Wang J, Cao Y, Ling J, Qian J, Lu Y, Li H, Zheng Y, Lan Y, Hong S, Matthews J, Starbuck MW, Navone NM, Orlowski RZ, Lin P, Kwak LW, Yi Q. 2012. Constitutive activation of p38 MAPK in tumor cells contributes to osteolytic bone lesions in multiple myeloma. Leukemia 26:2114–2123. https://doi.org/10.1038/leu.2012.71.
47. Puri PL, Wu Z, Zhang P, Wood LD, Bhakta KS, Han J, Feramisco JR, Karin M, Wang JY. 2000. Induction of terminal differentiation by constitutive activation of p38 MAP kinase in human rhabdomyosarcoma cells. Genes Dev 14:574–584.
48. Auger-Messier M, Accornero F, Goonasekera SA, Bueno OF, Lorenz JN, van Berlo JH, Willette RN, Molkentin JD. 2013. Unrestrained p38 MAPK activation in Dusp1/4 double-null mice induces cardiomyopathy. Circ Res 112:48–56. https://doi.org/10.1161/CIRCRESAHA.112.272963.
49. Han J, Lee JD, Jiang Y, Li Z, Feng L, Ulevitch RJ. 1996. Characterization of the structure and function of a novel MAP kinase kinase (MKK6). J Biol Chem 271:2886–2891. https://doi.org/10.1074/jbc.271.6.2886.
50. Pramanik R, Qi X, Borowicz S, Choubey D, Schultz RM, Han J, Chen G. 2003. p38 isoforms have opposite effects on AP-1-dependent transcription through regulation of c-Jun. The determinant roles of the isoforms in the p38 MAPK signal specificity. J Biol Chem 278:4831–4839. https://doi.org/10.1074/jbc.M207732200.
51. Cong L, Ran FA, Cox D, Lin S, Barretto R, Habib N, Hsu PD, Wu X, Jiang W, Marraffini LA, Zhang F. 2013. Multiplex genome engineering using CRISPR/Cas systems. Science 339:819–823. https://doi.org/10.1126/science.1231143.
52. Mali P, Yang L, Esvelt KM, Aach J, Guell M, DiCarlo JE, Norville JE, Church GM. 2013. RNA-guided human genome engineering via Cas9. Science 339:823–826. https://doi.org/10.1126/science.1232033.
53. Wu X, Tian L, Li J, Zhang Y, Han V, Li Y, Xu X, Li H, Chen X, Chen J, Jin W, Xie Y, Han J, Zhong CQ. 2012. Investigation of receptor interacting protein (RIP3)-dependent protein phosphorylation by quantitative phosphoproteomics. Mol Cell Proteomics 11:1640–1651. https://doi.org/10.1074/mcp.M112.019091.